Quantum mechanical simulation of crystaline systems

Roberto Dovesi

Gruppo di Chimica Teorica
Dip. Di Chimica IFM
Università degli Studi di Torino

Why simulation?

Is simulation useful?

Does it produce reasonable numbers?

Or can only try to reproduce the experiments?

Connected question:

Is simulation expensive?

How many transistors on a chip?

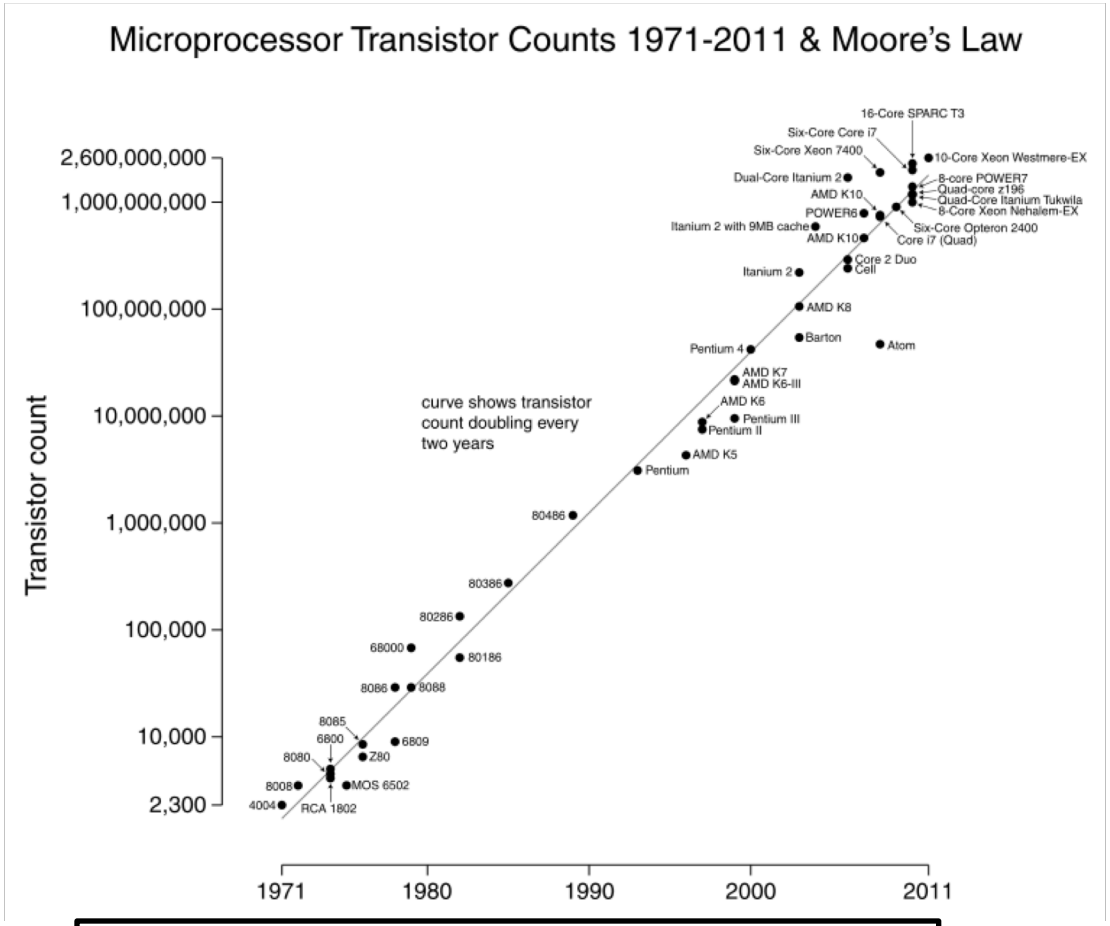

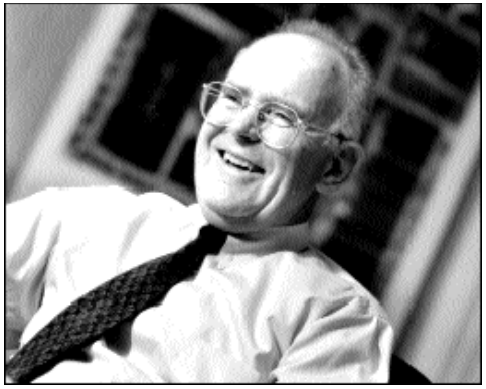

Gordon Moore

The number of transistors per chip doubles every 18 months

Performance of HPC

Keith E. Gubbins* and Joshua D. Moore *Ind. Eng. Chem. Res.* **2010,** *49,* 3026–3046

Molecular Modeling of Matter: Impact and Prospects in Engineering

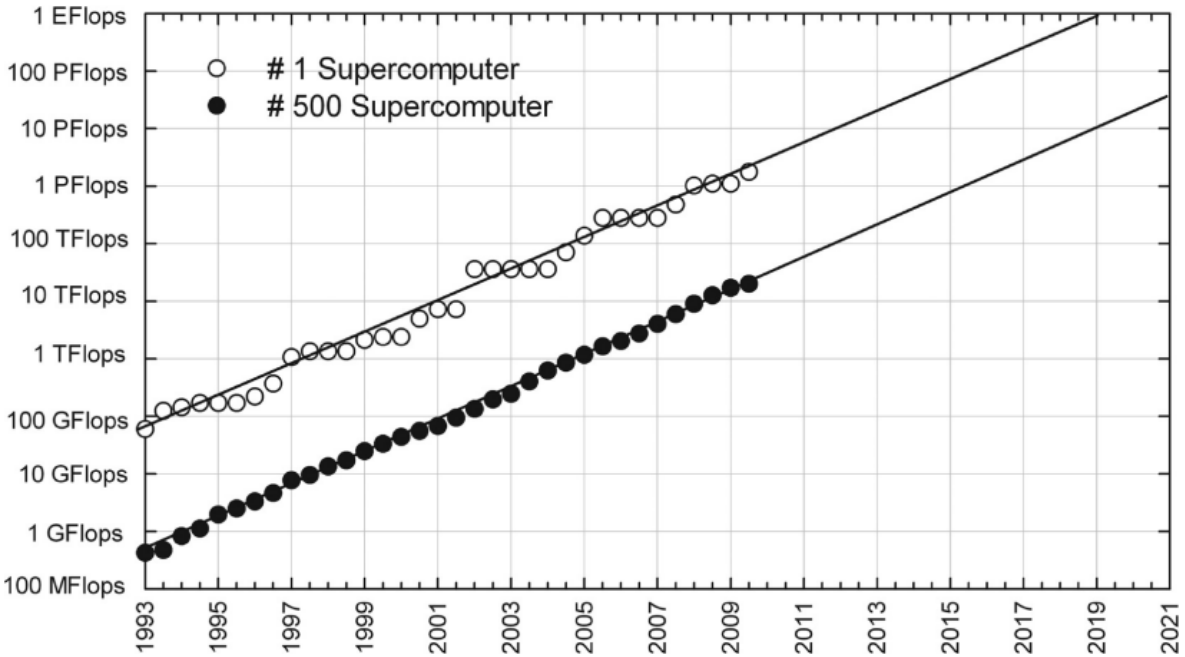

Figure 15. Top supercomputer in world versus the 500th supercomputer based on speed from June 1993 to November 2009 from the TOP500 list (a new lists appear in June and November of each year). Lines are drawn for the eye and serve as an estimate of possible future projections based on the data. (Data used with permission from TOP500 Supercomputing Sites, http://top500.org).

But…..

The evolution of the hardware is always much faster than that of the software.
Parallel computing….

How to fill supercomputers?

Is simulation expensive?
The last computer we bought….

Server Supermicro 64 CORE OPTERON euros 6.490 ,00

1 x Chassis 2U - 6 x SATA/SAS - 1400W

4 x CPU AMD Opteron 16-Core 6272 2,1Ghz 115W

8 x RAM 8 GB DDR3-1333 ECC Reg. (1GB/core)

1 x Backplane SAS/SATA 6 disks

1 x HDD SATAII 500 GB 7.200 RPM hot-swap

1 x SVGA Matrox G200eW 16MB

2 x LAN interface 1 Gbit

1 x Management IPMI 2.0

Cheap… but 64 cores-→ Parallel computing

Much less than most of the experimental equipments

64 cores enough for large calculation……..

At the other extreme: SUPERCOMPUTERS

Available, but:

a) They are fragile

b) Not so much standard (compiler, libreries)

c) The software (that is always late with respect to hardware) MUST BE ABLE TO EXPLOIT this huge power

The PRACE Tier-0 Resources

HORNET (HLRS, DE)
Cray XC30 system - 94,656 cores

CURIE (GENCI, FR)
BULL x86 system – 80,640 cores (thin nodes)

FERMI (CINECA, IT)
BlueGene Q system – 163,840 cores

PRACE

JUQUEEN (JÜLICH, DE)
BlueGene Q system – 458,752 cores

SUPERMUC (LRZ, DE)
IBM System x iDataPlex
system– 155,656 cores

MARENOSTRUM (BSC, SP)
IBM System x iDataPlex
system– 48,448 cores

MPPCRYSTAL: strong scaling

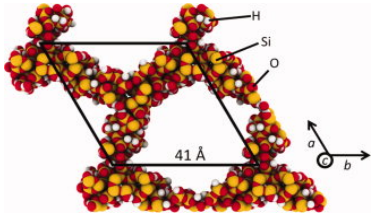

Scaling of **computational time** required for an SCF cycle with the number of processors for two supercells of mesoporous silica MCM-41, with a 6-31G** basis set and PBE functional. The X16 cell contains 9264 atoms and 124096 atomic orbitals, the X24 one 13896 atoms and 186144 atomic orbitals.

Various approaches can be used for the simulation of solids:

-classical or semi-classical energy expressions (force-field, electrostatic + repulsion terms);
structural, elastic, dielectric properties of ionic and semi-ionic compounds such as Al_2O_3 (corundum) or SiO_2 (quartz); the only available in the 1960-1980 period; still used for large systems or for a first quick determination. Parametric (then boring parametrization, usually valid for interpolation, much less for extrapolation……).

-MD (molecular dynamics) based on classical mechanics
(then on force fields). The only available for, say, more than 30.000 atoms (for example proteins). Temperature effect

Obviously no electronic wavefunction →
nothing about the related properties

Quantum mechanical

(based then on the solution of the Schroedinger equation at some level of approximation)

a) ab initio

(no parameters, also indicated as first-principle)

b) semi-empirical

in the quantum-mechanical frame many of the interactions (then of expensive integrals) are approximated with reference to some physical or chemical property. Cheaper than a)

Quantum mechanical, ab initio

I) wavefunction based (Hartree-Fock, Configuration interaction, Coupled Cluster, Moeller Plesset…..).

In short:

The multielectronic problem MUST be tackled through ONE electron wavefunctions: Hartree-Product >Slater Determinant >variational principle > double infinite expansion (basis set and determinants).

Historically, the Molecular or Chemistry approach.

Standard codes since 1960-70 (IBMOL- means IBM first explicit set of atomic wave-functions,
1974, Clementi and Roetti.
Gaussian (Pople) code (1975), and others in the following years.

Quantum mechanical, ab initio

II) Electronic Density based

(a 3 variables problem instead of 3N variables)

The Hohenberg-Kohn Theorems (1964) originates the DFT (Density Functional Theory):

LDA, GGA, meta-GGA, «hybrids», range separated……

a sort of medioeval «bestiarium»

because:

the theorems say that the TOTAL ENERGY (a number) only depends on the density (a function);

however the link between the two is unknown (or known only in limiting cases as for the electron gas). In practice solves an equation very close to the one for the wavefunction.

Here we consider the

QUANTUM MECHANICAL ab initio

approach to the properties of crystalline compounds

only crystalline (means: periodic in 1, 2 3 directions)?

NO!

The same scheme applies to:
a) local defects (say vacancies in silicon)
b) desordered systems (say solid solutions)

The level of the theory:

non relativistic
Schroedinger equation
Born-Hoppeneimer approximation
single particle approximation
single determinant (Hartree-Fock or ….DFT)
variational principle
local basis set (LCAO)

An obvious statement:
also the simplest crystalline system is much more complicated than the simplest molecular system:

Accurate studies for the latter in the ’60
(H_2, methane,benzene)

The first ab initio calculations for solids appear in 1979-1980 (diamond)

Hystorically, two separated development lines:

Molecules (or finite systems):
HF based, a local basis set, all electron

Solids (infinite in three directions)
DFT, plane-waves, pseudopotential.

In the last say 10 years…..intersections…

The simulation at the
theoretical chemistry group in Torino

The CRYSTAL code

The CRYSTAL PROJECT:

was formulated in the 1972-76 years by
Cesare Pisani, Carla Roetti and **Roberto Dovesi,**
starting from the periodic Hartree Fock schemes proposed
in these years by various authors
(André, Del Re, Harris, Ladik, Euwema);

first "exercices" with periodic EHT, CNDO, MNDO

Then many other contributions (local and from abroad)

Cesare Pisani

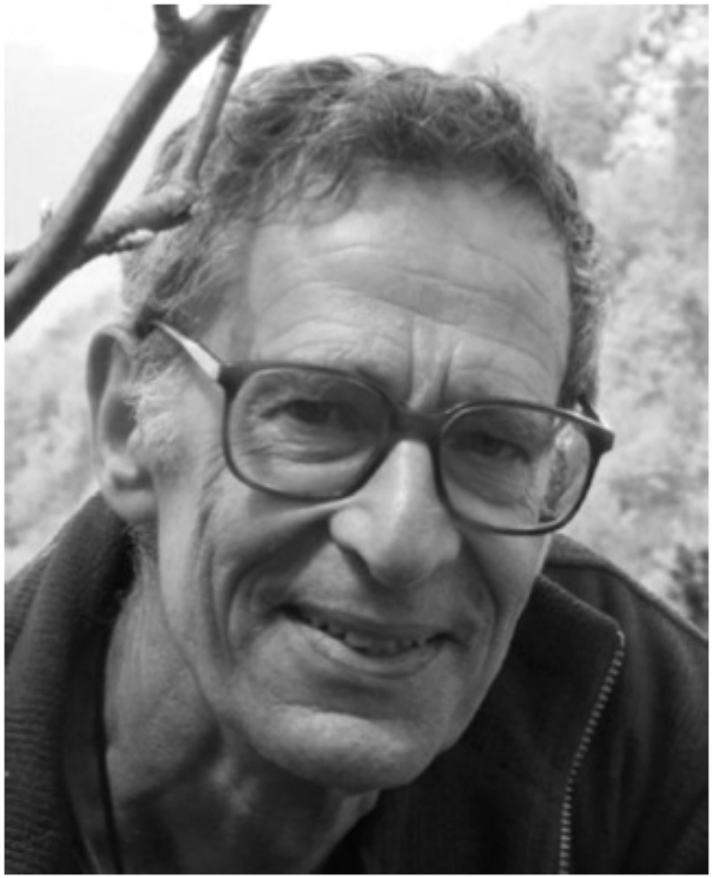

1938-2011

Cesare Pisani died on July 17, 2011,
in a mountains accident

Carla Roetti

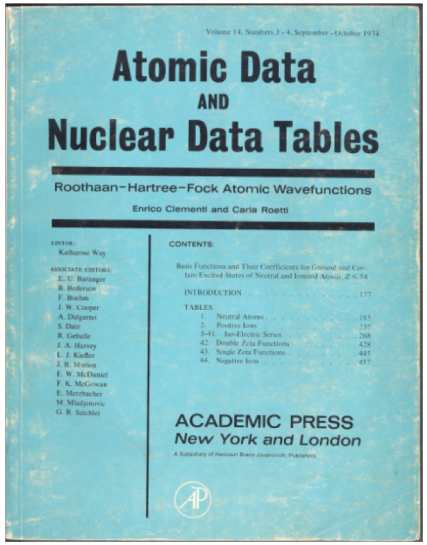

Carla Roetti graduated in chemistry (1967) from the University of Torino, where she became Associate Professor in Physical Chemistry in 1980.

Throughout her scientific career, she has been one of the leaders of the Theoretical Chemistry Group of the Torino University. For almost forty years (1974-2010) she has been involved with her colleagues in the quantum mechanical ab-initio study of the electronic properties of solids and in the implementation of related algorithms and computer codes, in particular of CRYSTAL.

Her contribution in this respect has been invaluable. Since the release of the first public version of CRYSTAL (1988) and throughout all the subsequent ones, she has played a leading rôle in the maintenance, portability, documentation and testing of the new features of the code, and the support of the users.

Carla Roetti has died on September 7th 2010,

all those who have worked and interacted with her deeply miss her.

The CRYSTAL code

for the investigation of systems periodic in 1D (polymers, nanotubes), 2D (monolayers, slabs), 3D (bulk)

Born in Torino in 1976, public releases in
1988 (QCPE),
1992, 1995, 1998, 2002, 2006, 2009,
2014

Contributions from many researchers
from many countries

CRYSTAL88,
was the first ab initio code publicly
available to the scientific community,

last release: 2014.

The basis set

The basis set consists of Bloch Functions (BF) defined in terms of local functions, the atomic orbitals (AO), $\chi_\mu(\mathbf{r})$, throughout the entire lattice ($\mathbf{g}$ = lattice vector):

$$\Phi_\mu(\mathbf{r};\mathbf{k}) = \sum_{\mathbf{g}}^{\infty} e^{i\,\mathbf{k}\cdot\mathbf{g}}\,\chi_\mu(\mathbf{r}-\mathbf{R}_\mu-\mathbf{g}) = \sum_{\mathbf{g}}^{\infty} e^{i\,\mathbf{k}\cdot\mathbf{g}}\,\chi_\mu^{\mathbf{g}}(\mathbf{r})$$

The local functions are, in turn, a linear combination of n_G individually normalized Gaussian type functions (GTF) with constant coefficients d_j and exponents α_j

$$\chi_\mu(\mathbf{r}-\mathbf{R}_\mu-\mathbf{g}) = \sum_{j}^{n_G} d_j\,G(\alpha_j;\mathbf{r}-\mathbf{R}_\mu-\mathbf{g})$$

Matrix elements of Fock matrix in direct space

$$F^{\mathbf{g}}_{\mu\nu} = T^{\mathbf{g}}_{\mu\nu} + Z^{\mathbf{g}}_{\mu\nu} + C^{\mathbf{g}}_{\mu\nu} + X^{\mathbf{g}}_{\mu\nu}$$ Fock matrix

$$T^{\mathbf{g}}_{\mu\nu} = \left\langle \chi^{\mathbf{0}}_{\mu} \middle| \hat{T} \middle| \chi^{\mathbf{g}}_{\nu} \right\rangle$$ kinetic contribution

$$Z^{\mathbf{g}}_{\mu\nu} = \left\langle \chi^{\mathbf{0}}_{\mu} \middle| \hat{Z} \middle| \chi^{\mathbf{g}}_{\nu} \right\rangle$$ electron-nuclei

$$C^{\mathbf{g}}_{\mu,\nu} = \sum_{\lambda,\rho}^{m} \sum_{n}^{\infty} P^{\mathbf{n}}_{\lambda,\rho} \sum_{\mathbf{h}}^{\infty} [(\chi^{\mathbf{0}}_{\mu}\chi^{\mathbf{g}}_{\nu}|\chi^{\mathbf{h}}_{\lambda}\chi^{\mathbf{h+n}}_{\rho})]$$ Coulomb el-el

$$X^{\mathbf{g}}_{\mu,\nu} = \sum_{\lambda,\rho}^{m} \sum_{\mathbf{n}}^{\infty} P^{\mathbf{n}}_{\lambda,\rho} \sum_{\mathbf{h}}^{\infty} [-\frac{1}{2}(\chi^{0}_{\mu}\chi^{\mathbf{h}}_{\lambda}|\chi^{\mathbf{g}}_{\nu}\chi^{\mathbf{h+n}}_{\rho})]$$ exchange el-el

$$P^{\mathbf{n}}_{\lambda,\rho} = 2 \int_{BZ} d\mathbf{k}\ e^{i\mathbf{k}.\mathbf{n}} \sum_{j} c_{\lambda,j}(\mathbf{k})\ c^{*}_{\rho,j}(\mathbf{k})\ \theta[\varepsilon_{Fermi} - \varepsilon_{j}(\mathbf{k})]$$

Integration in $\mathbf{k}$ space to compute the value of ε_{Fermi}

Hartree-Fock total energy per unit cell

$$E^{\text{electronic}} = E^{\text{mono}} + E^{\text{Coulomb}} + E^{\text{exchange}}$$

$$E^{\text{mono}} = \frac{1}{2} \sum_{\mu,\nu}^{m} \sum_{\mathbf{g}}^{\infty} P^{\mathbf{g}}_{\mu,\nu} \left\langle \chi^{\mathbf{0}}_{\mu} \left| \nabla^2 + \sum_{N}^{nuclei} \frac{Z_N}{r_N} \right| \chi^{\mathbf{g}}_{\nu} \right\rangle$$

$$E^{\text{Coulomb}} = \frac{1}{2} \sum_{\mu,\nu}^{m} \sum_{\mathbf{g}}^{\infty} P^{\mathbf{n}}_{\mu,\nu} \sum_{\lambda,\rho}^{m} \sum_{\mathbf{n}}^{\infty} P^{n}_{\lambda,\rho} \sum_{\mathbf{h}}^{\infty} [(\chi^{\mathbf{0}}_{\mu} \chi^{\mathbf{g}}_{\nu} \mid \chi^{\mathbf{h}}_{\lambda} \chi^{\mathbf{h+n}}_{\rho})]$$

$$E^{\text{exchange}} = \frac{1}{4} \sum_{\mu,\nu}^{m} \sum_{\mathbf{g}}^{\infty} P^{\mathbf{g}}_{\mu,\nu} \sum_{\lambda,\rho}^{m} \sum_{\mathbf{n}}^{\infty} P^{\mathbf{n}}_{\lambda,\rho} \sum_{\mathbf{h}}^{\infty} [(\chi^{\mathbf{0}}_{\mu} \chi^{\mathbf{h}}_{\lambda} \mid \chi^{\mathbf{g}}_{\nu} \chi^{\mathbf{h+n}}_{\rho})]$$

The evaluation of HF total energy of a periodic system requires the evaluation of 3 infinite summations ($\mathbf{h}$, $\mathbf{g}$, $\mathbf{n}$) that extend to all direct lattice vectors

Schrödinger equation in the BF basis

In the basis of Bloch functions the Hamiltonian matrix is factorized into diagonal blocks of finite size (the number of BFs in the unit cell), each corresponding to a point in reciprocal space.

Schrödinger equation can be solved independently at each $\mathbf{k}$ point.

$$H(\mathbf{k})\, C(\mathbf{k}) = S(\mathbf{k})\, C(\mathbf{k})\, E(\mathbf{k})$$

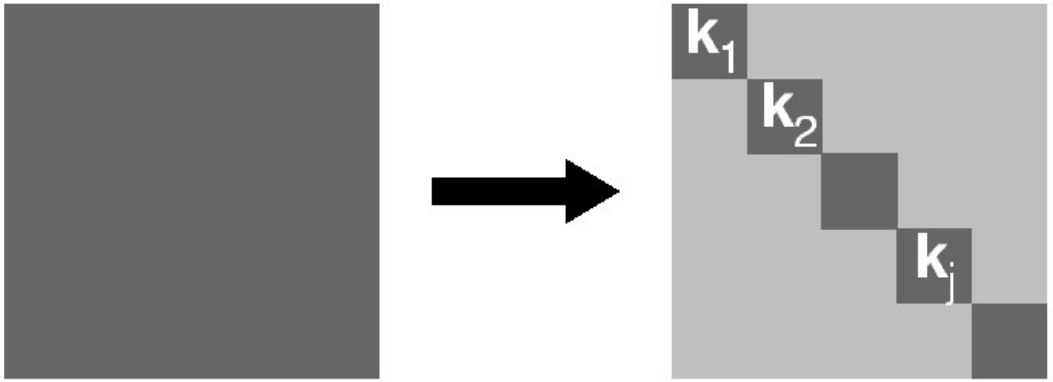

Symmetry Adapted Crystalline Orbitals

Some $\mathbf{k}$ points are invariant to some point symmetry operations: this property is used to generate Symmetry Adapted Bloch Functions from a set of local functions (AO).

The method, based on the diagonalization of Dirac characters, permits to factor out $\mathrm{H}(\mathbf{k})$ into smaller diagonal blocks:

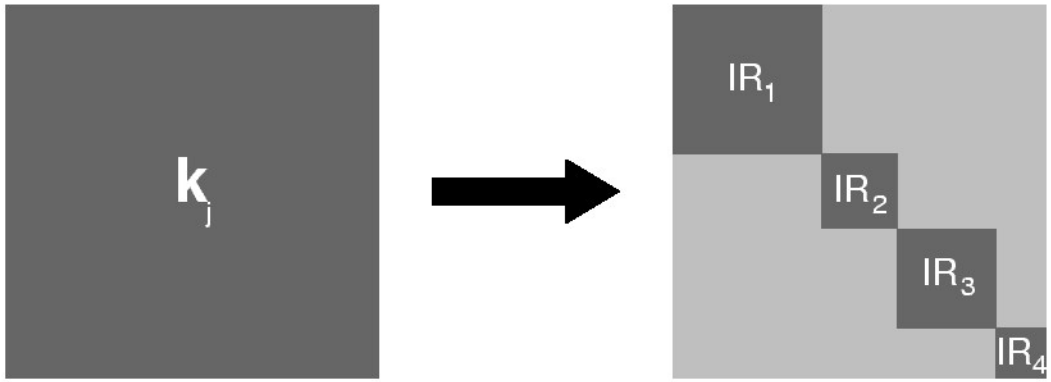

Hamiltonians

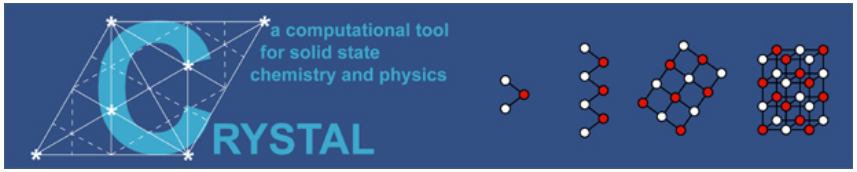

- **Restricted and Unrestricted Hartree-Fock Theory**
- **Total and Spin Density Functional Theory**

Local functionals [L] and gradient-corrected [G] exchange-correlation functionals

Exchange functionals

- Slater [L]
- von Barth-Hedin [L]
- Becke '88 [G]
- Perdew-Wang '91 [G]
- Perdew-Burke-Ernzerhof [G]
- **Revised PBE for solids [G]**
- **Second-order GGA expansion for solids [G]**
- **Wu-Cohen '06 [G]**

Correlation functionals

- Vosko-Willk-Nusair (VWN5 parameterization) [L]
- Perdew-Wang [L]
- Perdew-Zunger '81 [L]
- von Barth-Hedin [L]
- Lee-Yang-Parr [G]
- Perdew '86 [G]
- Perdew-Wang '91 [G]
- Perdew-Burke-Ernzerhof [G]
- **Revised PBE for solids [G]**
- **Wilson-Levy '90 [G]**

Types of calculations

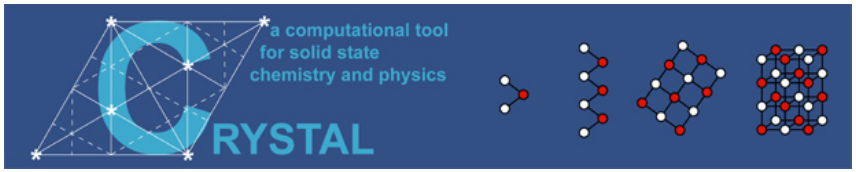

- **Single-point energy calculation**
- **Automated geometry optimization**
  - Full geometry optimization (cell parameters and atom coordinates)
  - Freezes atoms during optimization
  - **Constant volume or pressure constrained geometry optimization**
  - **Transition state search**
- **Harmonic vibrational frequencies**
  - Frequencies at Γ point
  - **Phonon dispersion with an efficient supercell approach**
  - IR intensities through either localized Wannier functions or **Berry phase scheme**
  - **Reflectance spectrum**
  - Exploration of the energy and geometry along selected normal modes
- **Anharmonic frequencies for X-H bonds**

A few applications…….

Total energy calculation….
Geometry optimization….

CRAMBIN

Crambin is a small seed storage protein from the Abyssinian cabbage. It belongs to thionins. It has **46 aminoacids (642 atoms)**.

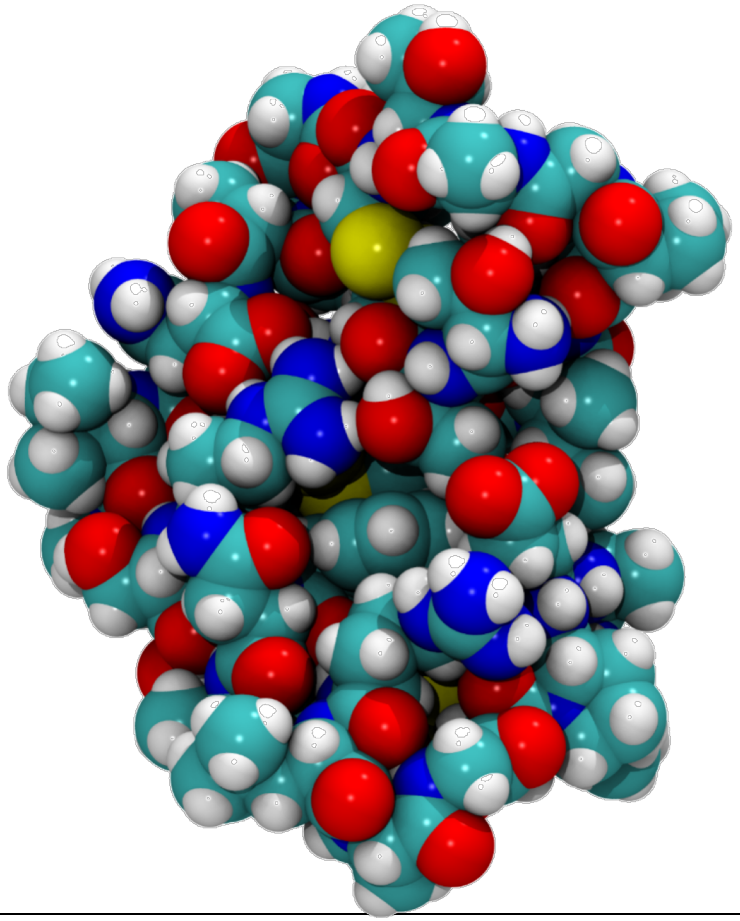

Primary structure:

Secondary structure:

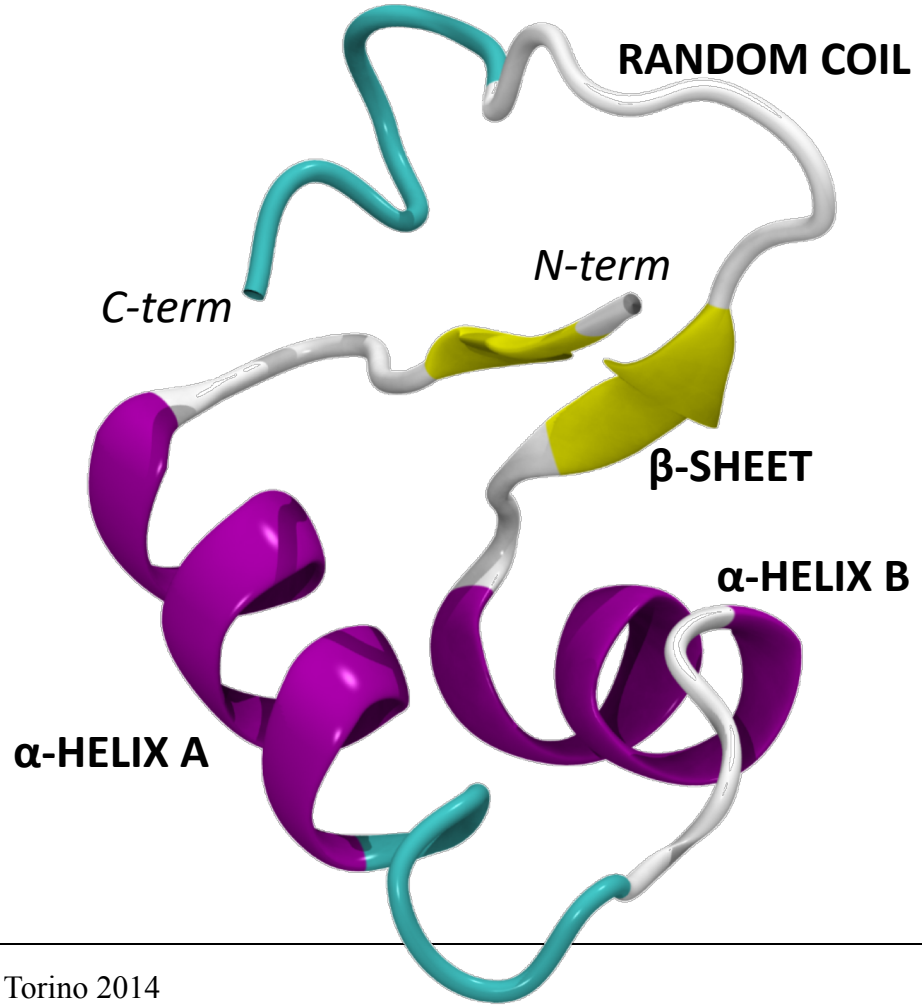

Tensorial Properties of Crystals

Second order	*Third order*	*Fourth order*
Dielectric Polarizability	Piezoelectric First hyperpolarizability	Elastic Photoelastic Second hyperpolarizability

Maximum number of independent elements according to crystal symmetry:

6	18	21

Minimum number of independent elements according to crystal symmetry:

1	1	3

Effect of the Crystal Symmetry on Tensors

Third Order Tensors:

Triclinic

Class *1*

(18)

Hexagonal

Class *6*

(4)

same as class *4*

Cubic

Classes $\bar{4}3m$ and *23*

(1)

Fourth Order Tensors:

Triclinic

Both classes

(21)

Hexagonal

All classes

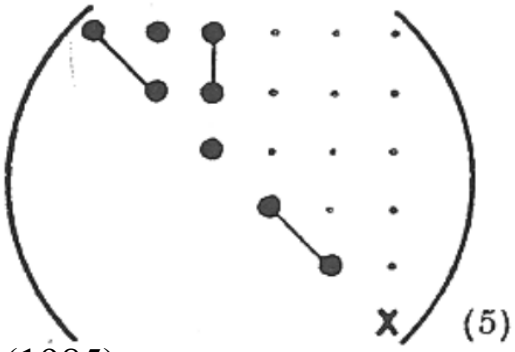

(5)

Cubic

All classes

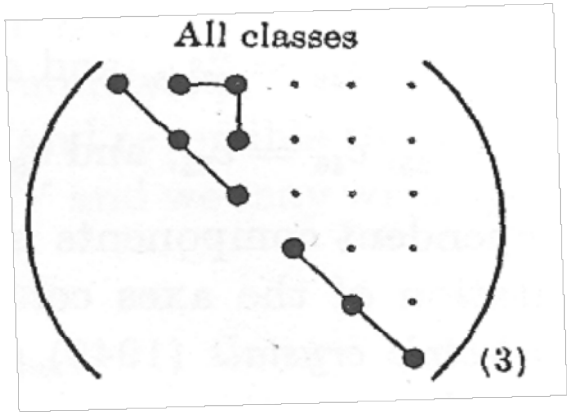

(3)

J. F. Nye, *Oxford University Press*, (1985)

Tensorial Properties Related to Crystal Strain

Elastic Tensor	Piezoelectric Tensor	Photoelastic Tensor
$C_{vu} = \frac{1}{V} \frac{\partial^2 E}{\partial \epsilon_v \partial \epsilon_u}\Big\|_0$	$e_{iv} = \frac{\partial P_i}{\partial \epsilon_v}\Big\|_0$	$p_{ijv} = \frac{\partial \Delta \epsilon_{ij}^{-1}}{\partial \epsilon_v}$
4	**3**	**4**

Order of the Tensors

Second derivatives of the total energy *E* with respect to a pair of strains, for a 3D crystal	First derivative of the polarization **P** (computed through the Berry phase approach) with respect to the strain	First derivative of the inverse dielectric tensor (difference with respect to the unstrained configuration) with respect to strain

Voigt's notation is used according to *v, u* = 1, . . . 6 (1 = xx, 2 = yy, 3 = zz, 4 = yz, 5 =xz, 6 = xy) and *i,j* =1, 2, 3 (1 = x , 2 = y, 3 = z).

Tensorial Properties Related to Crystal Strain

Elastic Tensor

$$C_{vu} = \frac{1}{V} \left. \frac{\partial^2 E}{\partial \epsilon_v \partial \epsilon_u} \right|_0$$

Geometry definition
ELASTCON
[Optional keywords]
END
END
Basis set definition
END
Comput. Parameters
END

Piezoelectric Tensor

$$e_{iv} = \left. \frac{\partial P_i}{\partial \epsilon_v} \right|_0$$

Geometry definition
PIEZOCON
[Optional keywords]
END
END
Basis set definition
END
Comput. Parameters
END

Photoelastic Tensor

$$p_{ijv} = \frac{\partial \Delta \epsilon_{ij}^{-1}}{\partial \epsilon_v}$$

Geometry definition
PHOTOELA
[Optional keywords]
END
END
Basis set definition
END
Comput. Parameters
END

CRYSTAL14: Elastic Properties

Pyrope-$Mg_3Al_2(SiO_4)_3$

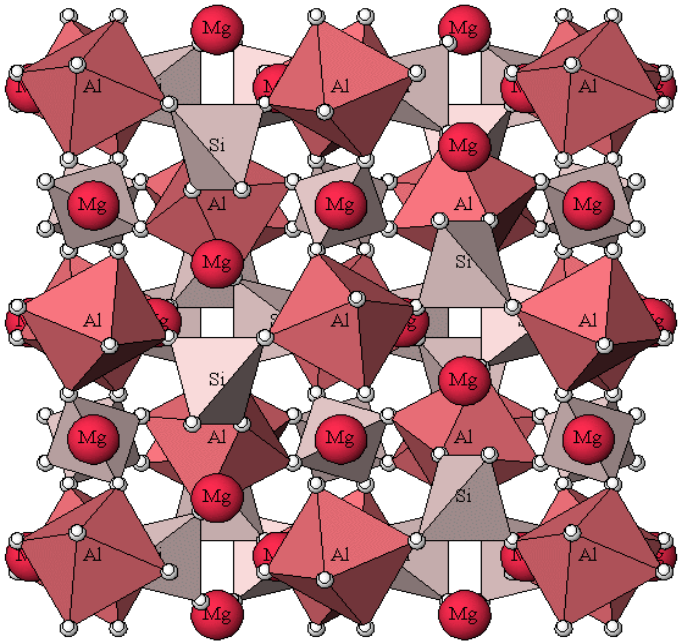

Table 1 Elastic constants C_{vu} (GPa) and adiabatic bulk modulus K_S (GPa) of the six silicate garnet end-members here considered. Present computed values are compared with previously measured experimental (above the horizontal line) and simulated (below lines) data.

		C_{11}	C_{12}	C_{44}	K_S
Pyr	Isaak *et al.* (1976)	287	105	92	166
	Bonczar *et al.* (1977)	292	106	92	168
	Leitner *et al.* (1980)	295	117	90	177
	O'Neill *et al.* (1989)	296	111	92	173
	O'Neill *et al.* (1991)	298	110	93	172
	Sinogeikin *et al.* (2000)	297	108	93	171
	Lu *et al.* (2013)	291	107	92	168
	Pavese (1999)	298	113	93	174
	Winkler *et al.* (1999)	339	132	115	201
	Mittal *et al.*(2001)	314	116	91	182
	This study	**296**	**109**	**89**	**171**

A. Erba, A. Mahmoud, R. Orlando and R. Dovesi, *Phys. Chem. Minerals* (2013)
DOI 10.1007/s00269-013-0630-4

CRYSTAL14: Elastic Properties

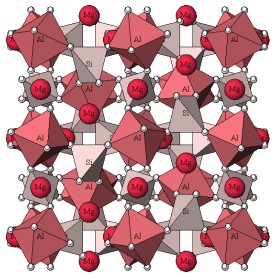

Pyrope

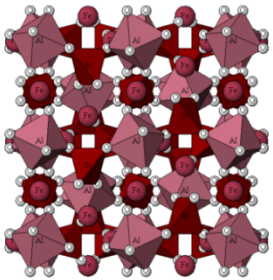

Almandine

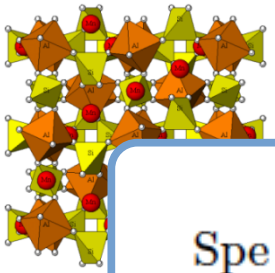

Spessartine

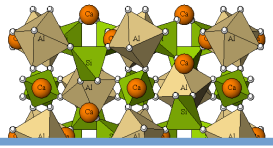

Grossular

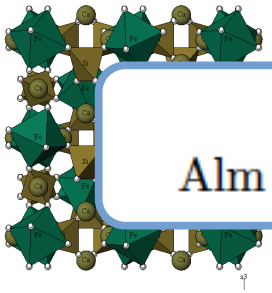

Andradite

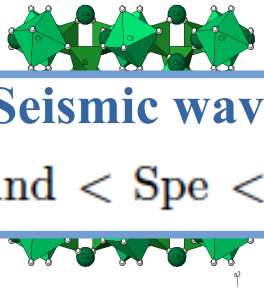

Uvarovite

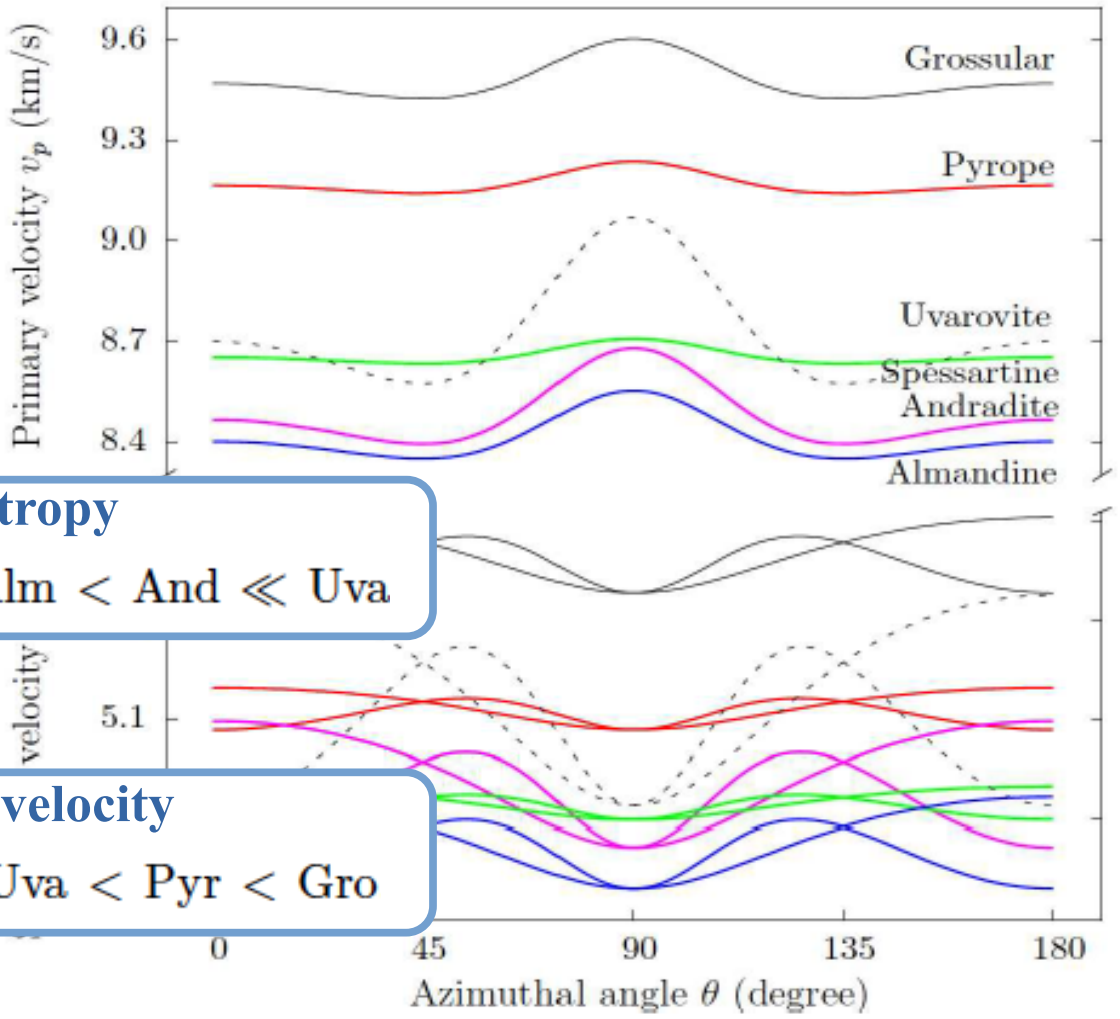

Elastic Anisotropy

Spe < Pyr < Gro < Alm < And ≪ Uva

Seismic wave velocity

Alm < And < Spe < Uva < Pyr < Gro

A. Erba, A. Mahmoud, R. Orlando and R. Dovesi, *Phys. Chem. Minerals* (2013)
DOI 10.1007/s00269-013-0630-4

CRYSTAL14: Piezoelectric and Dielectric Properties

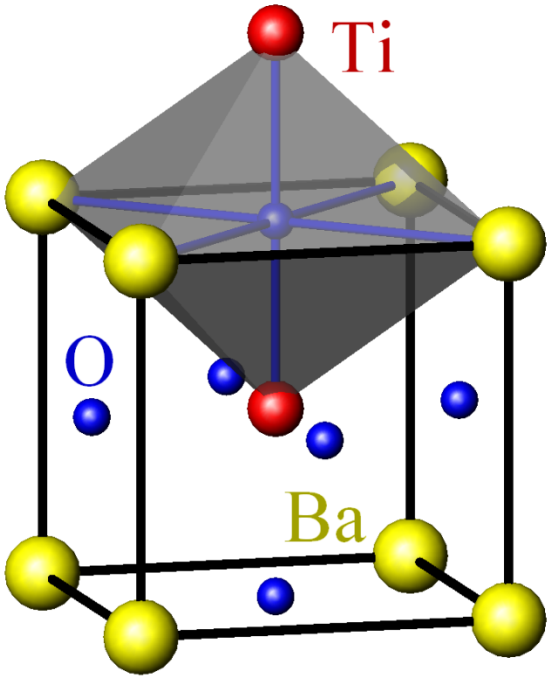

TABLE V: Direct and converse piezoelectric constants of the rhombohedral phase of $BaTiO_3$, as computed with four different Hamiltonians. Electronic and total nuclear relaxed values are given.

	Direct (C/m^2)				Converse (pm/V)			
	e_{15}	e_{21}	e_{31}	e_{33}	d_{15}	d_{21}	d_{31}	d_{33}
HF								
Relaxed	-7.52	3.24	-3.30	-4.41	1562†	-511†	-9.2	-15.6
Clamped	0.14	-0.19	0.06	-0.14	1.6	-0.8	0.2	-0.4
LDA								
Relaxed	-5.81	3.75	-4.77	-6.46	-95.0	30.3	-8.7	-16.8
Clamped	0.13	-0.15	0.04	-0.12	1.1	-0.6	0.2	-0.4
PBE								
Relaxed	-4.31	1.93	-2.11	-3.52	-290	80.6	-5.2	-14.1
Clamped	0.20	-0.28	0.05	-0.23	2.5	-1.4	0.3	-0.9
PBE0								
Relaxed	-4.67	1.99	-2.17	-3.45	-271	73.9	-5.0	-12.2
Clamped	0.21	-0.28	0.06	-0.22	2.3	-1.2	0.3	-0.8

† These unusual large values are due to very large elements of the HF compliance tensor $\mathbb{S} = \mathbb{C}^{-1}$ in this case.

A. Mahmoud, A. Erba, Kh. E. El-Kelany, M. Rérat and R. Orlando, *Phys. Rev. B* (2013)

CRYSTAL14: Photoelastic Properties

The three independent elasto-optic constants of MgO, computed at PBE level, as a function of the electric field wavelength λ

p_{44} is almost wavelength independent

p_{11} and p_{12} show a clear dependence from λ

Dashed vertical lines in the figure identify the experimental range of adopted electric field wavelengths

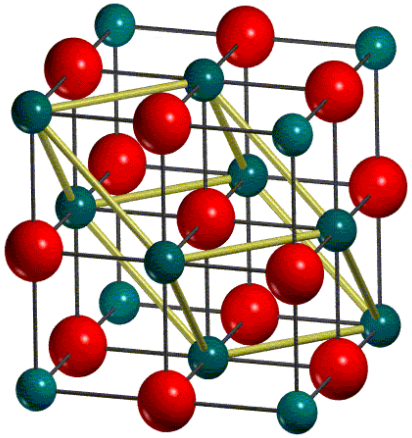

TABLE IV: Elasto-optic constants of the MgO crystal as experimentally measured by various workers, compared with the results of the present study.

	$p_{11}-p_{12}$	p_{44}	p_{11}	p_{12}
Giardini *et al.*[68]	-0.25	-0.10	-0.21	+0.04
Vedam *et al.*[10]	-0.248	×	-0.259	-0.011
Burstein *et al.*[71]	-0.24	×	-0.3	-0.08
Krishna Rao *et al.*[72]	-0.24	-0.105	-0.31	-0.07
West *et al.*[73]	-0.253	-0.096	×	×
Present work LDA	-0.231	-0.075	-0.218	+0.013
Present work PBE	-0.228	-0.078	-0.213	+0.015

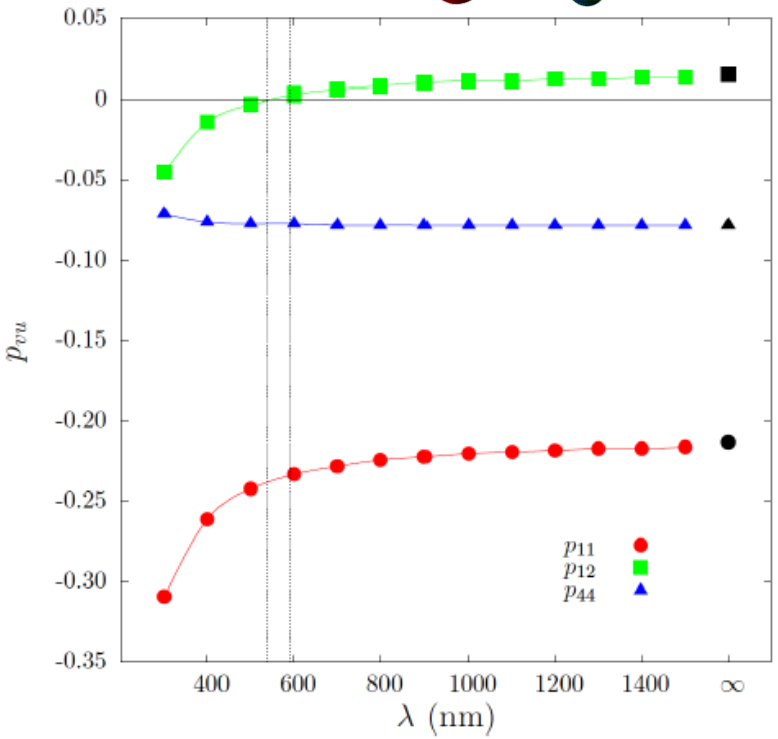

A. Erba and R. Dovesi, *Phys. Rev. B* ***88,*** 045121 (2013)

Vibrational properties

IR and Raman spectra……

Garnets: $X_3Y_2(SiO_4)_3$

X	**Y**	**Name**
Mg	Al	Pyrope
Ca	Al	Grossular
Fe	Al	Almandine
Mn	Al	Spessartine
Ca	Fe	Andradite
Ca	Cr	Uvarovite

Space Group: Ia-3d

80 atoms in the primitive cell (240 modes)

$\Gamma^{rid} = \mathbf{3A_{1g}} + 5A_{2g} + \mathbf{8E_g} + 14\,F_{1g} + \mathbf{14\,F_{2g}} + 5A_{1u} + 5\,A_{2u} + 10E_u + \mathbf{18F_{1u}} + 16F_{2u}$

17 IR ($\mathbf{F_{1u}}$) and 25 RAMAN ($\mathbf{A_{1g}}$, $\mathbf{E_g}$, $\mathbf{F_{2g}}$) active modes

Silicate garnet spessartine structure: $Mn_3Al_2(SiO_4)_3$

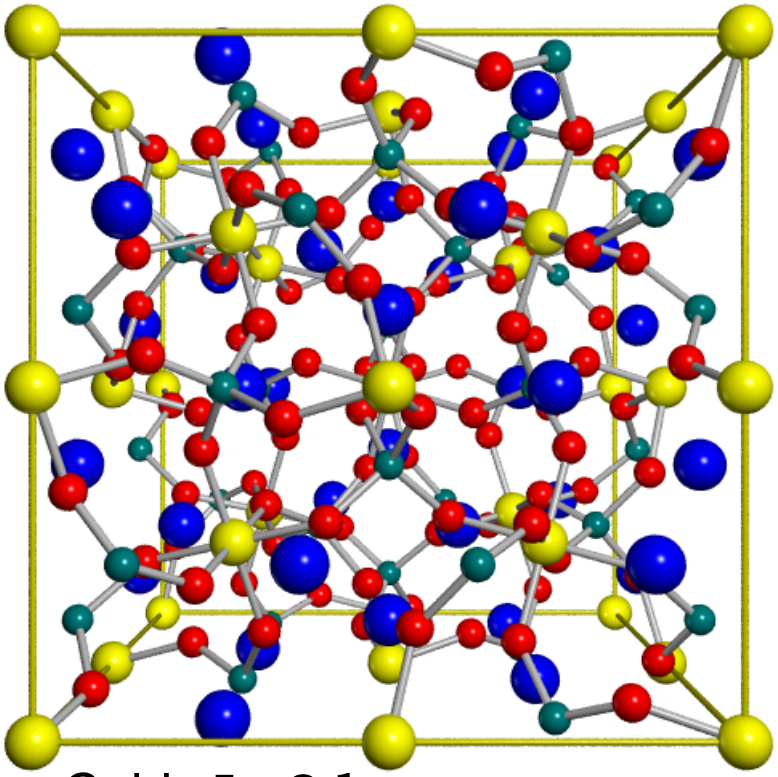

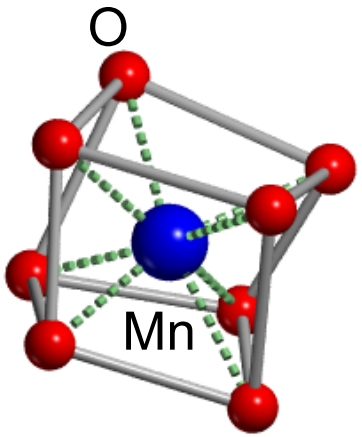

distorted dodecahedra

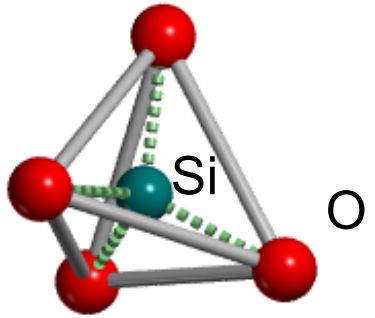

tetrahedra

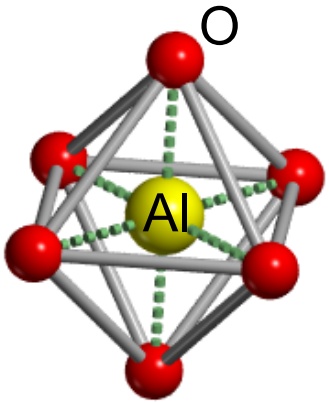

octahedra

- Cubic **Ia-3d**
- 160 atoms in the UC (80 in the primitive)
- O general position (48 equivalent)
- Mn (24e) Al (16a) Si (24d) site positions

Harmonic frequency in solids with CRYSTAL

Building the Hessian matrix

$$v_j = \frac{\partial V}{\partial u_j}$$

analytical first derivative

$$H_{ji} = \left[\frac{\partial v_j}{\partial u_i}\right]_0 \approx \frac{v_j(0,\ldots,u_i,\ldots) - v_j(0,\ldots,-u_i,\ldots)}{2u_i}$$

numerical second derivative

$$W_{ij}(k=0) = \sum_G \frac{H_{ij}^{0G}}{\sqrt{M_i M_j}}$$

Harmonic frequencies at the central zone are obtained by diagonalising the mass weighted Hessian matrix, W

Isotopic shift can be calculated at no cost!

Spessartine raman modes : Calc vs Exp

Calculated Modes BSB			Observed Modes	
			Exp. a)	Exp. b)
	υ	Δυ a)	υ	υ
F_{2g}	1033	-4	1029	1027
E_{2g}	914	-1	913	913
A_{2g}	910	-5	905	905
F_{2g}	877	2	879	878
E_{2g}	852	-	-	892
F_{2g}	845	4	849	849
F_{2g}	640	-10	630	628
E_{2g}	596	-4	592	5920
F_{2g}	588	-15	573	573
A_{2g}	561	-9	552	550
E_{2g}	531	-9	522	521
F_{2g}	505	-5	500	499
F_{2g}	476	-1	475	472

Frequency differences (Δυ) are evaluated with respect to experimental data. υ and Δυ in cm^{-1}.

a) Hofmeister &Chopelas, Phys. Chem Min. 1991

b) Kolesov &Geiger, Phys. Chem. Min.1998

Spessartine raman modes : Calc vs Exp

Calculated Modes BSB			Observed Modes	
			Exp. a)	Exp. b)
	υ	Δυ a)	υ	υ
E_{2g}	376	-4	372	372
F_{2g}	366	-	-	-
F_{2g}	348	2	350	350
A_{2g}	342	8	350	347
E_{2g}	320	1	321	318
F_{2g}	315	13	302	314
E_{2g}	299	-30	269	-
F_{2g}	221	0	221	229
F_{2g}	195	1	196	194
F_{2g}	165	10	175	163
E_{2g}	163	-1	162	162
F_{2g}	105	-	-	-

Frequency differences (Δυ) are evaluated with respect to experimental data. υ and Δυ in cm^{-1}.

Garnets : Statistics

IR frequencies

	n. of compared ν	TO			LO		
		$\overline{\lvert\Delta\rvert}$	$\overline{\Delta}$	$\lvert\Delta_{max}\rvert$	$\overline{\lvert\Delta\rvert}$	$\overline{\Delta}$	$\lvert\Delta_{max}\rvert$
Pyrope[a]	17+17	6.0	-1.0	23.3	6.8	-2.8	23.3
Grossular[b]	16+16	3.4	-0.8	8.6	5.1	-2.0	28.2
Almandine[a]	17+17	5.5	1.6	21.1	3.9	0.6	12.7
Spessartine[c]	17+17	4.2	-2.4	11.0	3.4	0.0	8.6
Andradite[b]	17+17	7.3	-7.3	13.7	6.2	-6.2	12.0
Uvarovite[d]	5+5	4.0	-1.8	6.5	3.8	-2.0	6.3
TOTAL	89+89	5.2	-2.0	23.3	5.0	-2.1	28.2

Raman frequencies[e]

	$\overline{\lvert\Delta\rvert}$	$\overline{\Delta}$	$\lvert\Delta_{max}\rvert$
Pyrope	7.6	-3.2	31
Grossular	7.5	3.0	32
Almandine	4.2	0.7	17
Spessartine	6.8	0.6	30
Andradite	5.3	-5.1	11
Uvarovite	4.6	-0.4	22

a) Hofmeister et al., *Phys. Chem. Min.* **1996.** *81*, 418

b) McAloon et. al., *Phys. Chem. Min*. **1995.** *80*, 1145

c) Hofmeister et. al., *Phys. Chem. Min*. **1991.** *17*, 503

d) Hofmeister, private comm.

e) Kolesov et. al., *Phys. Chem. Min*. **1998.** *25*, 142

Statistical analysis of calculated IR and Raman modes of garnets compared to experimental data.

IR reflectance spectrum

Reflectivity is calculated from dielectric constant by means of:

$$R(\nu) = \left| \frac{\sqrt{\epsilon(\nu) - \sin^2\theta} - \cos\theta}{\sqrt{\epsilon(\nu) - \sin^2\theta} + \cos\theta} \right|^2$$

(θ is the beam incident angle)

The **dielectric function** is obtained with the classical dispersion relation:

$$\epsilon(\nu) = \epsilon_\infty + \sum_j \frac{f_j \nu_j^2}{\nu_j^2 - \nu^2 - i\nu\gamma_j}$$

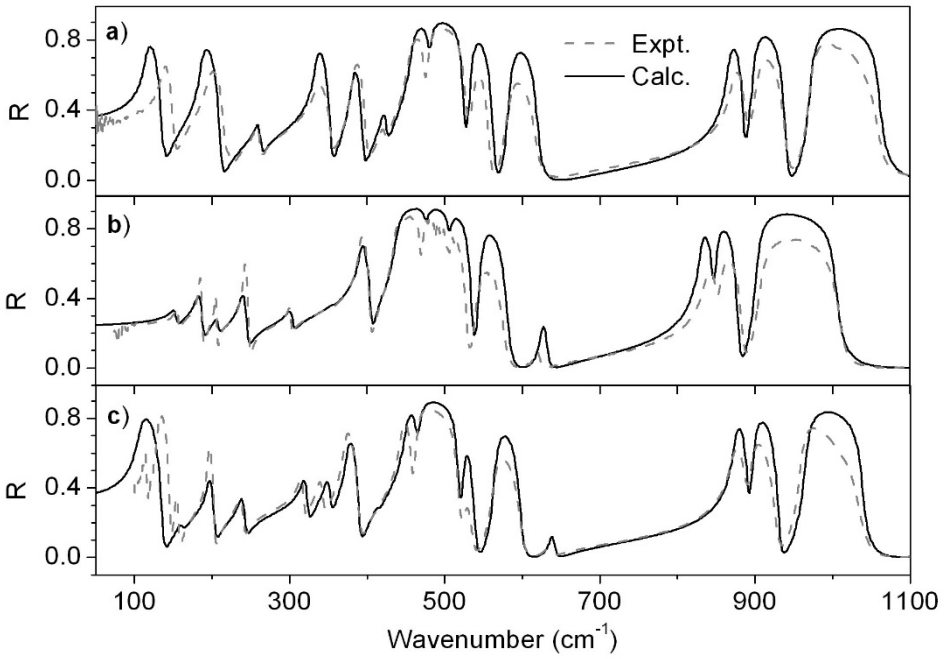

Comparison of computed and experimental IR reflectance spectra for garnets: a) pyrope b) grossular c) almandine .

IR reflectance spectrum of grossular

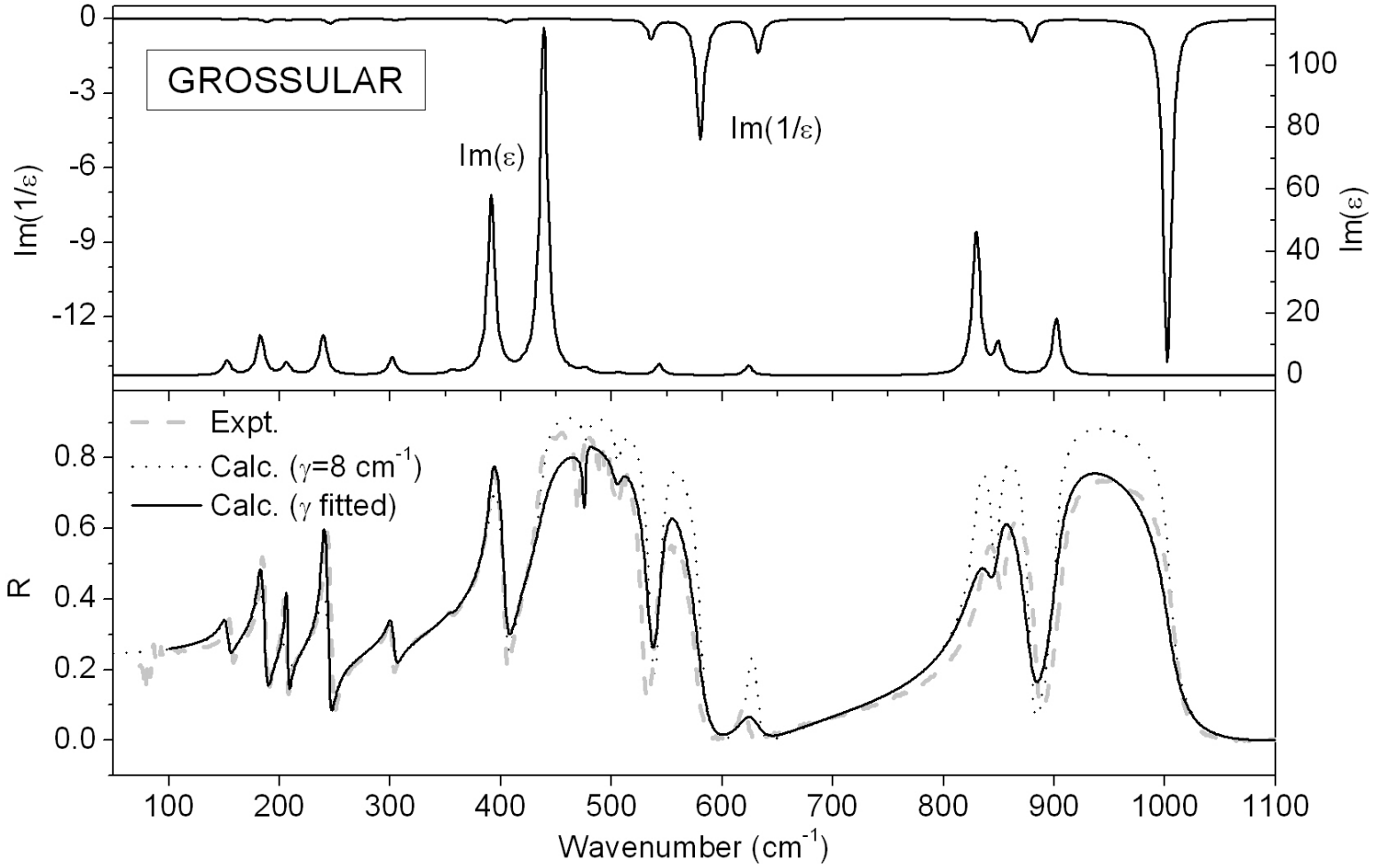

Computed and experimental IR reflectance spectra of grossular garnet, plus imaginary parts of ε and 1/ε.

IR reflectance spectrum: required quantities

- **Optical dielectric constant ε^{∞}**
  - Computed through a Coupled Perturbed HF(KS) scheme

	Calc.	Exp.	Δ%
Pyrope	2.74	3.06	-12
Grossular	2.78	2.96	-7
Almandine	3.23		
Spessartine	3.08	3.24	-5
Andradite	3.40	3.53	-4
Uvarovite	3.24	3.42	-6

Optical dielectric constants of garnets
(expt. from Medenbach et al., *J. Opt. Soc.Am. B*, **1997**, 14, 3299-3318)

- **Transverse Optical vibrational frequencies ν**
  - Eigenvalues of the Hessian matrix, constructed in the harmonic approximation
- **Damping factors γ**
  - A constant value 8 cm^{-1} is adopted

The RAMAN spectrum of Pyrope:

25 modes

From A_{1g}+E_g wavenumbers...

		Ours	Hofmeister		Chopelas		Kolesov	
Sym	*M*	υ (cm^{-1})	υ (cm^{-1})	Δυ (cm^{-1})	υ (cm^{-1})	Δυ (cm^{-1})	υ (cm^{-1})	Δυ (cm^{-1})
A_{1g}	*1*	352.5	362	-10	362	-10	364	-12
	2	564.8	562	3	562	3	563	2
	3	926.0	925	1	925	1	928	-2
E_g	*4*	209.2	203	6	203	6	211	-2
	5	308.5			**309**	-1	284	25
	6	336.5	342	-6			344	-8
	7	376.9	365	12	**379**	-2	375	2
	A		439		439			
	8	526.6	524	3	524	3	525	2
	9	636.0	626	10	626	10	626	10
	10	864.4			**867**	-3		
	B		911					
	11	937.4	938	-1	938	-1	945	-8

Frequency differences are evaluated with respect to **calculated data**.

Hofmeister: Hofmeister & Chopelas, *Phys. Chem. Min.*, 1991

Chopelas: Chaplin & Price & Ross, *Am. Mineral.*, 1998

Kolesov: Kolesov & Geiger, *Phys. Chem. Min.*, 1998

... to RAMAN spectra!

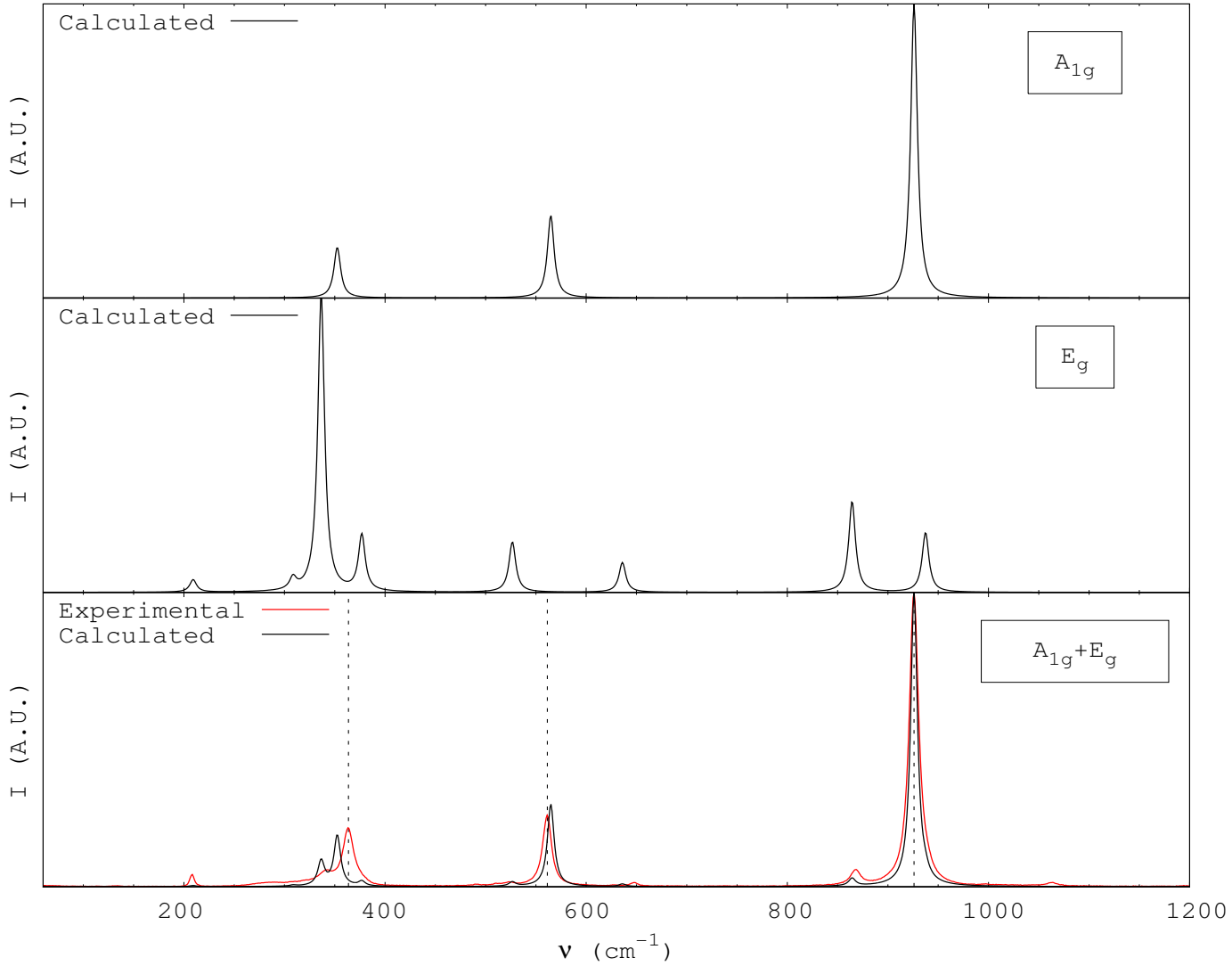

And now F_{2g} wavenumbers...

		Ours	Hofmeister		Chopelas		Kolesov	
Sym.	*M*	υ (cm-1)	υ (cm-1)	Δυ (cm-1)	υ (cm-1)	Δυ (cm-1)	υ (cm-1)	Δυ (cm-1)
F_{2g}	*12*	97.9	-	-	-	-	135	-37
	13	170.1	-	-	-	-	-	-
	14	203.7	208	-4	208	-4	212	-8
	C		230		230			
	15	266.9	272	-5	272	-5	-	-
	D		285					
	16	319	318	1	**318**	1	322	-3
	E				**342**			
	17	350.6	350	1	350	1	353	-2
	18	381.9	379	3	379	3	383	-1
	19	492.6	490	3	490	3	492	1
	20	513.5	510	4	510	4	512	2
	21	605.9	598	8	598	8	598	8
	22	655.3	648	7	648	7	650	5
	23	861	866	-5	866	-5	871	-10
	24	896.7	899	-2	899	-2	902	-5
	25	1068.4	1062	6	1062	6	1066	2

B3LYP overstimates the lattice parameter!

Frequency differences are evaluated with respect to **calculated data**.

Hofmeister: Hofmeister & Chopelas, *Phys. Chem. Min.*, 1991

Chopelas: Chaplin & Price & Ross, *Am. Mineral.*, 1998

Kolesov: Kolesov & Geiger, *Phys. Chem. Min.*, 1998

... and the RAMAN spectra!

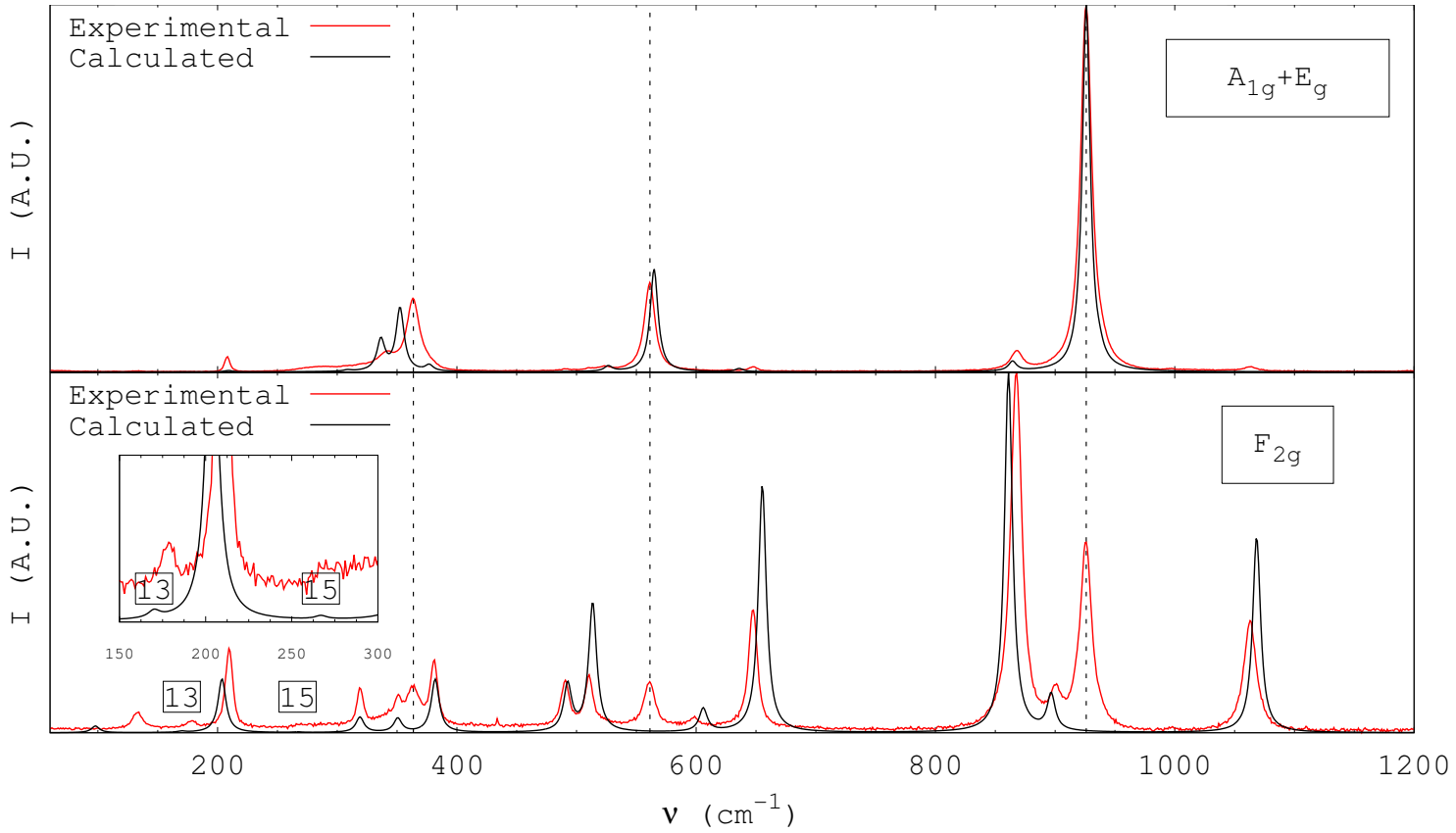

A_{1g} peaks also in **F_{2g}** spectrum caused by the presence of different crystal orientations and/or rotation of the polarized light.

High-order dielectric properties of solids

The total energy of a crystal in an electric field

The total energy (E_{tot}) of a crystal (or a molecule) in a "weak" electric field (ε) can be expressed as a perturbative series of the field components plus the total energy of the field-free system (E^0_{tot}):

$$E_{tot}(\varepsilon) = E^0_{tot} - \mu \cdot \varepsilon - \frac{1}{2!}\alpha\,\varepsilon^2 - \frac{1}{3!}\beta\,\varepsilon^3 - \frac{1}{4!}\gamma\,\varepsilon^4 - \ldots$$

$$\mu_t = -\left(\frac{\partial E_{tot}}{\partial \varepsilon_t}\right)_{\varepsilon=0}$$ dipole moment

$$\alpha_{tu} = -\left(\frac{\partial^2 E_{tot}}{\partial \varepsilon_t \partial \varepsilon_u}\right)_{\varepsilon=0}$$ polarizability

$$\beta_{tuv} = -\left(\frac{\partial^3 E_{tot}}{\partial \varepsilon_t \partial \varepsilon_u \partial \varepsilon_v}\right)_{\varepsilon=0}$$ first-order hyperpolarizability

$$\gamma_{tuvw} = -\left(\frac{\partial^4 E_{tot}}{\partial \varepsilon_t \partial \varepsilon_u \partial \varepsilon_v \partial \varepsilon_w}\right)_{\varepsilon=0}$$ second-order hyperpolarizability

The effect of a low-intensity high-frequency electric field (ε) applied to a crystal within the periodic boundary conditions can be represented by the following perturbative term in the Hamiltonian operator:

$$\Omega(\varepsilon, \mathbf{k}) = \varepsilon \cdot [\mathbf{r} + i\,\nabla_{\mathbf{k}}]$$

$\mathbf{r}$: position operator; $\nabla_{\mathbf{k}}$: gradient in **k** space

Ω depends on **k**, any point in the reciprocal space

Static polarizability and hyperpolarizabilities

$$\alpha_{tu} = -\frac{1}{n_k}\sum_{\mathbf{k}}^{BZ}\sum_{j}^{occ} P\Big[\overbrace{W_{jj}^{(tu)} + \sum_{\ell}^{virt}\Big(G_{j\ell}^{(t)}U_{\ell j}^{(u)} - U_{j\ell}^{(u)}G_{\ell j}^{(t)}}^{E_j^{(ut)}} \overbrace{- U_{j\ell}^{(u)\dagger}W_{\ell j}^{(t)} - W_{j\ell}^{(t)}U_{\ell j}^{(u)}\Big) - W_{jj}^{(tu)}}^{B_j^{(ut)}} \Big] =$$

$$= -\frac{2}{n_k}\sum_{\mathbf{k}}^{BZ}\sum_{j}^{occ}\sum_{\ell}^{virt} P\Re\left[\Xi_{j\ell}^{(t)}U_{\ell j}^{(u)}\right]$$

$$\beta_{tuv} = -\frac{1}{n_k}\sum_{\mathbf{k}}^{BZ}\sum_{j}^{occ}\sum_{\ell}^{virt} P\Re\left[G_{j\ell}^{(t)}U_{\ell j}^{(uv)} - W_{j\ell}^{(tu)}U_{\ell j}^{(v)}\right]$$

***n*+1 formulation**

substitute for $U^{[2]}$

$$\beta_{tuv} = -\frac{2}{n_k}\sum_{\mathbf{k}}^{BZ}\sum_{j}^{occ}\sum_{\ell}^{virt} P\Re\left[U_{j\ell}^{\dagger(t)}\left(\sum_{m}^{virt}G_{\ell m}^{(u)}U_{mj}^{(v)} - \sum_{m}^{occ}U_{\ell m}^{(v)}G_{mj}^{(u)} + i\frac{\partial U_{\ell j}^{(v)}}{\partial k_u}\right)\right]$$

2*n*+1 formulation

$$\gamma_{tuvw} = -\frac{1}{n_k}\sum_{\mathbf{k}}^{BZ}\sum_{j}^{occ}\sum_{\ell}^{virt} P\Re\Bigg[U_{j\ell}^{\dagger(t)}\Bigg(\sum_{m}^{all}G_{\ell m}^{(u)}U_{mj}^{(vw)} - \sum_{m}^{occ}U_{\ell m}^{(vw)}G_{mj}^{(u)} +$$

$$+\frac{1}{2}\sum_{m}^{virt}W_{\ell m}^{(uv)}U_{mj}^{(w)} - \frac{1}{2}\sum_{m}^{virt}U_{\ell m}^{(w)}E_{mj}^{(uv)}\Bigg) + iU_{j\ell}^{\dagger(vw)}\frac{\partial U_{\ell j}^{(t)}}{\partial k_u}\Bigg]$$

2*n*+1 formulation

Dielectric properties

Polarizability (α) and hyperpolarizability (β and γ) tensors are related to other tensors:

$$\chi^{(1)}_{tu} = \frac{4\pi}{V}\alpha_{tu}$$ first-order electric susceptibility

V = unit cell volume

$$\in_{tu} = \delta_{tu} + \chi^{(1)}_{tu}$$ dielectric tensor

δ = Kronecker delta

$$\chi^{(2)}_{tuv} = \frac{2\pi}{V}\beta_{tuv}$$ second-order electric susceptibility

$$d_{tuv} = \frac{\chi^{(2)}_{tuv}}{2}$$ second-harmonic generation (SHG) electric susceptibility

$$\chi^{(3)}_{tuvw} = \frac{2\pi}{3V}\gamma_{tuvw}$$ third-order electric susceptibility

Potassium Di-hydrogen Phosphate KDP

- Chemical formula: KH_2PO_4
- NonLinear Optic Properties (NLO):
  the electric polarization (P) shows a NON LINEAR optic response to the applied electric field (F).
- Ferroelectric Phase Transition (PARA->FERRO) at 123° K

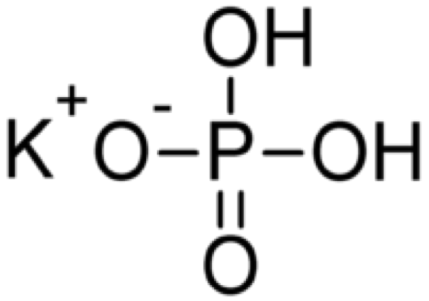

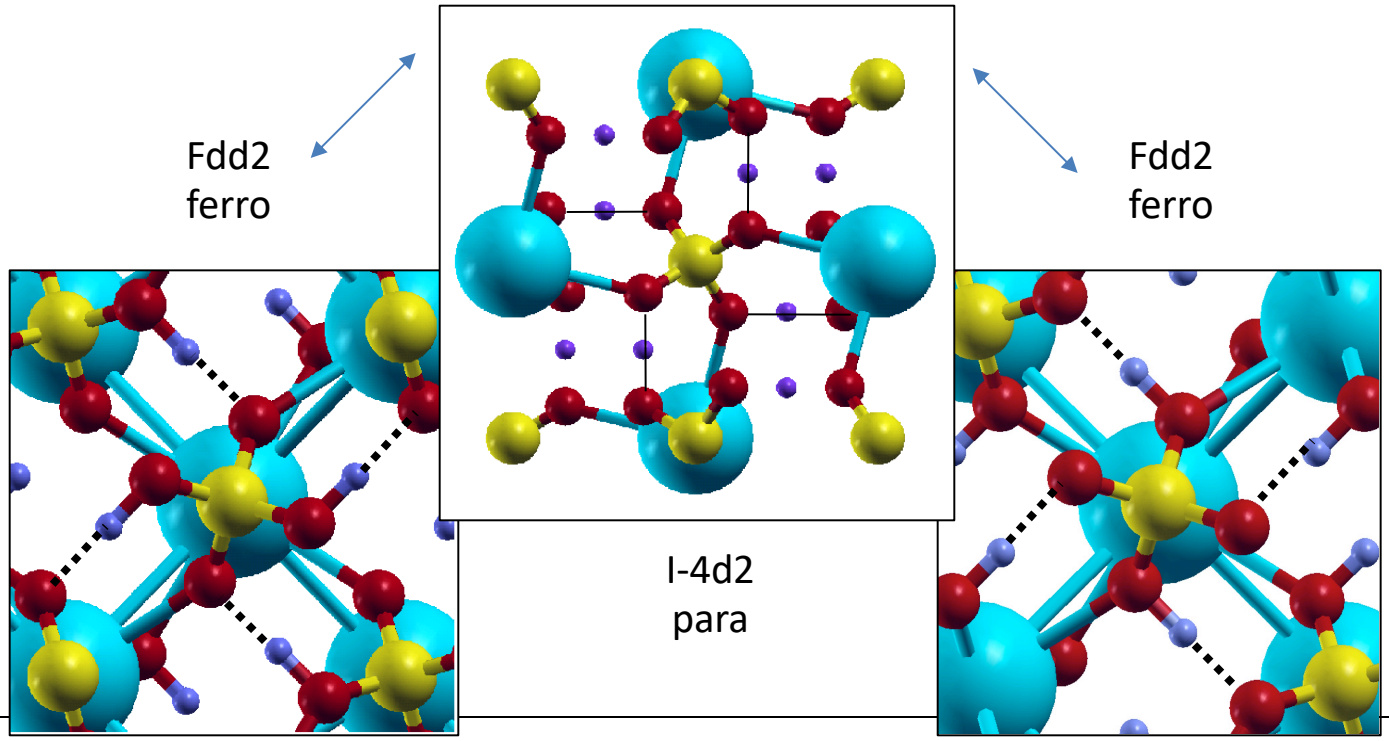

Potassium Di-hydrogen Phosphate KDP

Tetragonal (I-4d2)

- Symmetric H-bonds
- Above T_c: DISORDER, protons move along the H-bond (PE)
- Transition state as documented by negative frequencies.

Orthorhombic (Fdd2)

- Protonic Trasfer
- Below T_c: ORDER, protons fixed in ferroelectric domains (FE)
- Real minimum: all frequencies are positive

Potassium Di-hydrogen Phosphate KDP

K

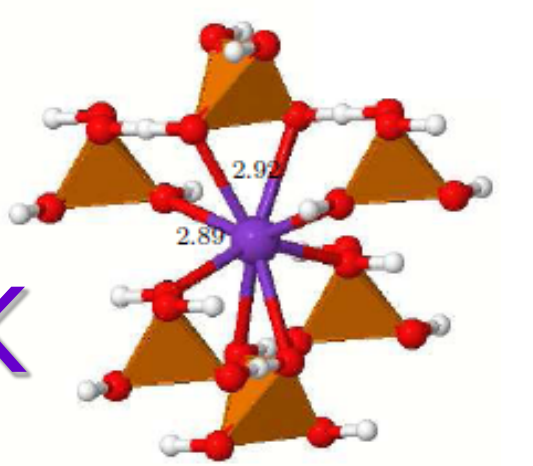

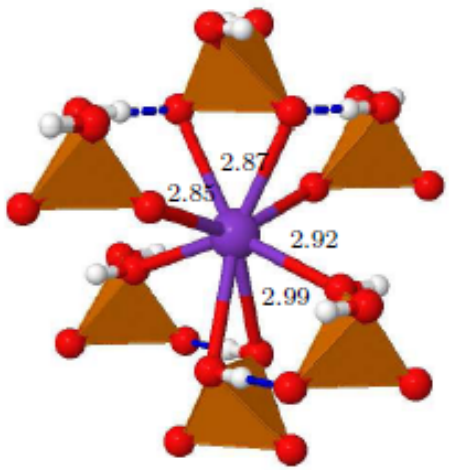

I-4d2 Fdd2

P

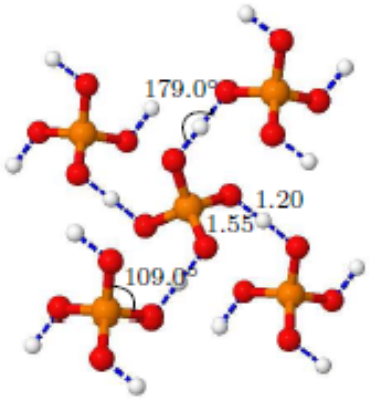

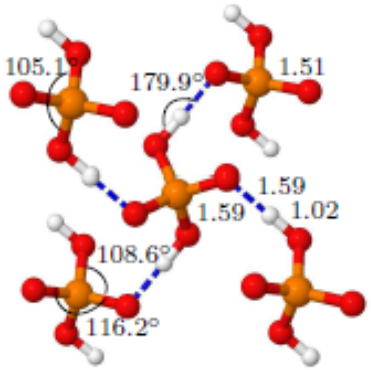

	I-4d2 (Exp)	Fdd2 (Exp.)
a	7.44 (7.44)	10.56 (10.53)
b	7.44 (7.44)	10.67 (10.44)
c	6.95 (6.97)	6.98 (6.90)
$H\text{-}O_1$	1.19 (1.25)	1.03 (1.05)
$H\text{-}O_2$	1.19 (1.25)	1.48 (1.44)
$P\text{-}O_1$	1.54 (1.54)	1.58 (1.59)
$P\text{-}O_2$	1.54 (1.54)	1.51 (1.50)

OPTGEOM: PBE0 [1]

1. V. Lacivita, M. Rérat, B. Kirtman, M. Ferrero, R. Orlando and R. Dovesi, J. Chem. Phys. 2009.

Potassium Di-hydrogen Phosphate KDP

		I-4d2 (Exp)	Fdd2 (Exp)
Dielectric Tensor (adimensional)	ε(xx)	2.23 (2.24)	2.18(2.26)
	ε(yy)	2.23 (2.24)	2.20(2.30)
	ε(zz)	2.05 (2.13)	2.06(2.16)
Second Harmonic Generation (SHG) coefficients (pm/V)	d(xxz)	0 (0)	0,389
	d(yyz)	0 (0)	-0,255
	d(zzz)	0 (0)	-0,018
	d(xyz)	0.37 (0.39)	0
Energy gap (eV)	G	7.99 (7.12)	7,97

CPHF: B3LYP, Exp. geom.

1. V. Lacivita, M. Rérat, B. Kirtman, M. Ferrero, R. Orlando and R. Dovesi, J. Chem. Phys. 2009.

Potassium Di-hydrogen Phosphate KDP

Dielectric Tensor and Optical Indicatrix

$$n = \sqrt{\epsilon}$$

- DIAGONALIZATION -> **PRINCIPAL REFRACTIVE INDICES** ($\alpha <= \beta <= \gamma$)
- **BIREFRINGENCE**: $B = \gamma - \alpha \ (\neq 0)$
- OPTICAL CLASSES:

1) **MONOAXIAL** = one monorefringence direction (one optical axis)

2) **BIAXIAL** = two monorefringence directions (two optical axes)

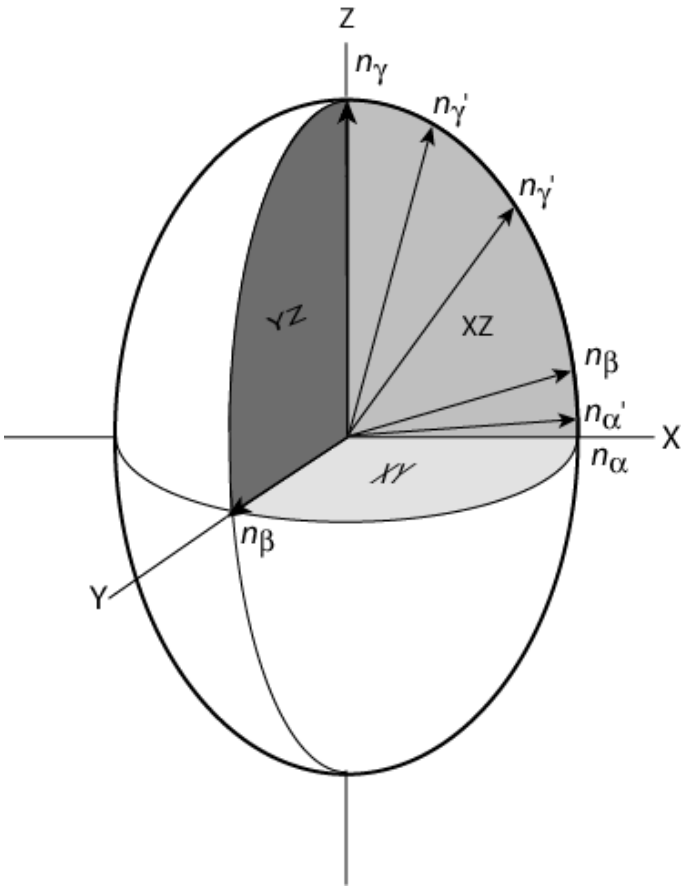

Potassium Di-hydrogen Phosphate KDP

Tetragonal (I-4d2)

- Monoaxial
- Oblate optical indicatrix

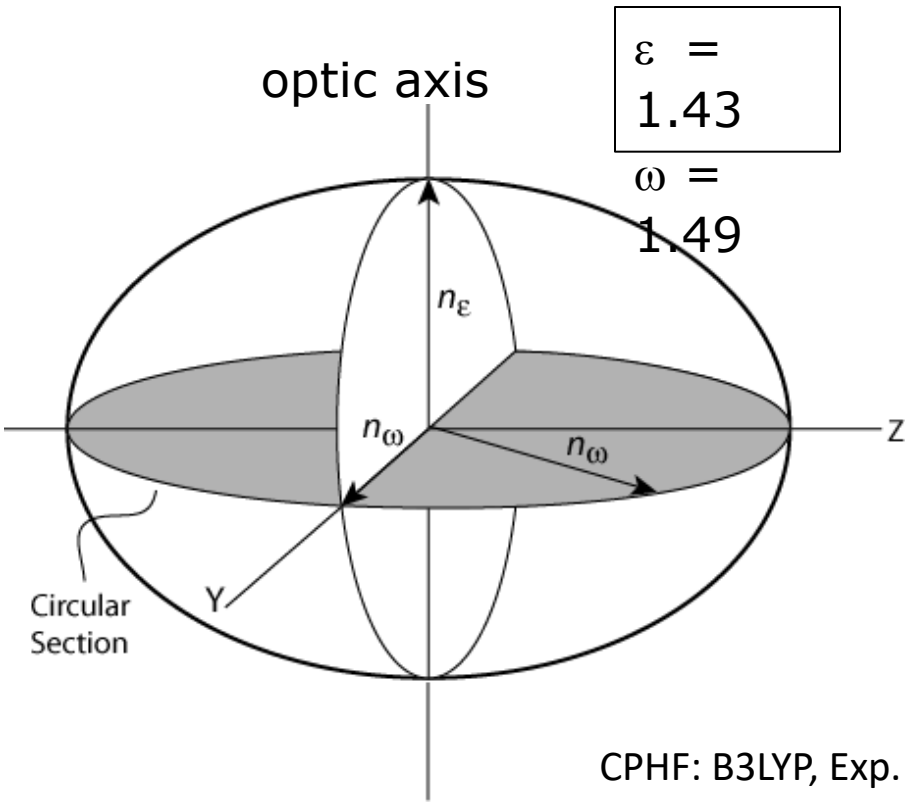

Orthorhombic (Fdd2)

- Biaxial

α = 1.436
β = 1.476
γ = 1.484

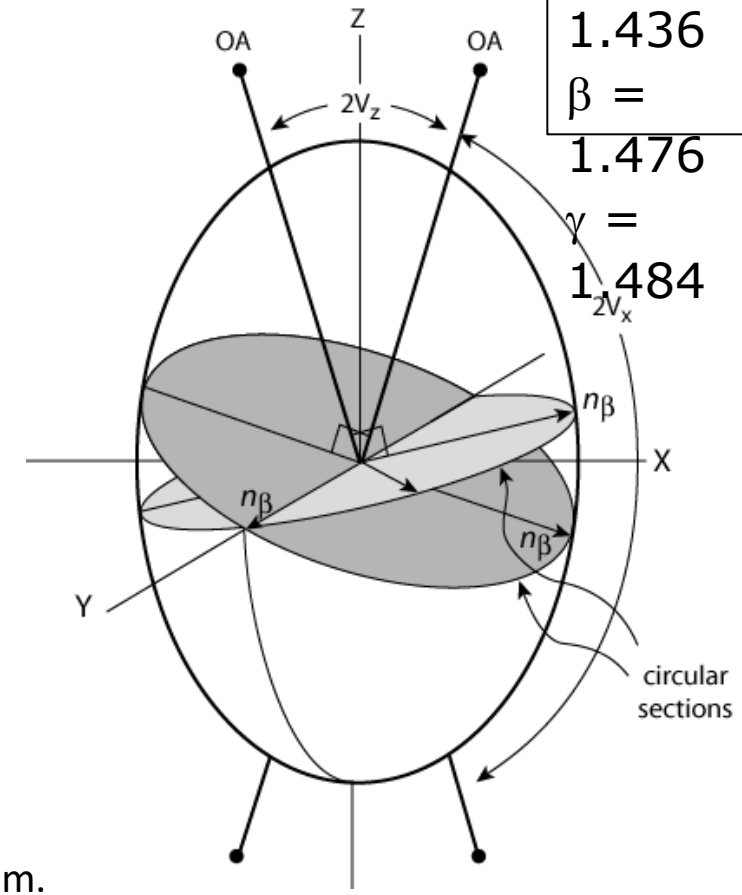

CPHF: B3LYP, Exp. geom.

Nanotubes

Nanotubes

What's new in the implemented method?

The **exploitation of the high point symmetry**
in helical 1D systems allows to
dramatically reduce the computational cost
and **automatically build nanotubes**
from 2D and 3D structures.

Y. Noël, P. D'Arco, R. Demichelis, C. M. Zicovich-Wilson, R.Dovesi; J. Comput. Chem., 2010, 31, 855-862

Why?

Nanotube ab initio simulation is, in general, **expensive**:
the unit cell can contain hundreds or thousands of atoms.

QM ab initio calculation of nanotubes with large basis sets and hybrid functionals: POSSIBLE AND NOT EXPENSIVE

Nanotubes

Automatic Construction of a Nanotube from 2D Structures

(CRYSTAL can authomatically cut 2D layers from 3D structures)

We start from 2D graphene, a simple case ---> C nanotube (CNT).

Shortest lattice vector perpendicular to ***R***:

$\boldsymbol{L}=l_1\boldsymbol{a_1}+l_2\boldsymbol{a_2}$

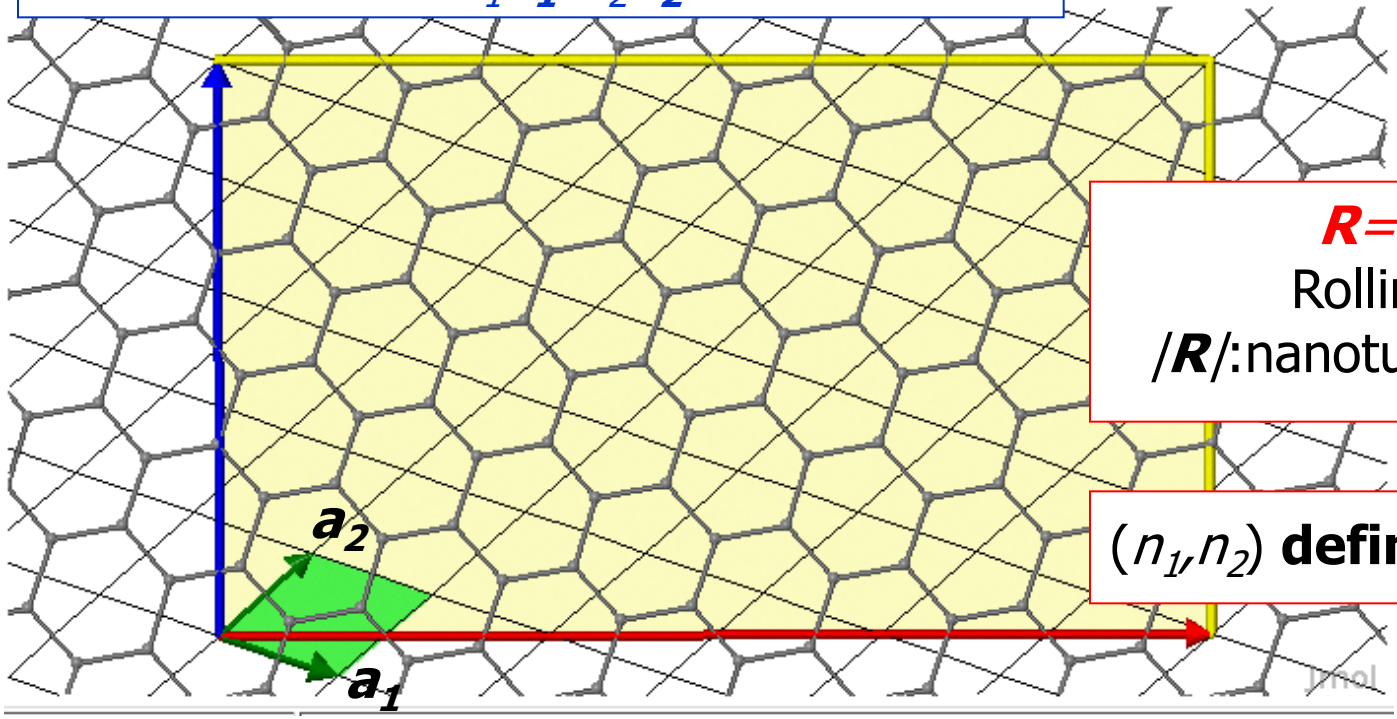

$\boldsymbol{R}=n_1\boldsymbol{a_1}+n_2\boldsymbol{a_2}$

Rolling direction

/***R***/:nanotube circumference

(n_1,n_2) **defines the nanotube**

* Noël, D'Arco, Demichelis, Zicovich-Wilson, Dovesi; J. Comput. Chem., 2010, 31, 855-862

Nanotubes

Exploitation of the High Point Symmetry of Nanotubes

A CNT unit cell can contain hundreds of atoms

BUT

ONLY 2 IRREDUCIBLE ATOMS WITH HELICAL SYMMETRY EXPLOITATION

EXAMPLE: frequency calculation of the (24,0) SWCNT

(96 atoms in the unit cell)

FREQUENCY CALCULATION:

- equilibrium geometry
- displacement of each atom along the 3 Cartesian directions

96x3+1=289 SCF calculations

If the calculation is performed on 2 irreducible atoms:

2x3+1=7 SCF calculations (helical symmetry exploitation)

* Noël, D'Arco, Demichelis, Zicovich-Wilson, Dovesi; J. Comput. Chem., 2010, 31, 855-862

Exploitation of the High Point Symmetry of Nanotubes

The helical symmetry of nanotubes is then exploited at three levels:

1 - Automatic generation of the nanotube starting from a 2D structure

- ✓ Easy to use
- ✓ Thick slabs can be treated
- ✓ Geometry guess for nanotubes

```
Build the (4,2) SWCNT
CRYSTAL
0 0 0
186
2.47 6.70
2
6 0.000000 0.000000 0.000000
6 0.333333 0.666667 0.000000
SLAB
0 0 1
1 1
SWCNT
4   2
```

3D geometry

Cut a slab

Build nanotube

* Noël, D'Arco, Demichelis, Zicovich-Wilson, Dovesi; J. Comput. Chem., 2010, 31, 855-862

Time Scaling

Single SCF step of (n,0) SW-CNT, n=8 to 24

N(AOs) : 704 to2112
Symmetry operators (N_S): 16 to 48

Time (24,0)<1.2 Time (8,0)

Gradient: same behavior as bi-electronic integrals, cost from (12,0) to (24,0) varies by less than 1%

Size of irreducible Fock matrix **roughly constant**

B3LYP, 6-1111G*
single processor Intel Xeon 1.86GHz, RAM 8Gb

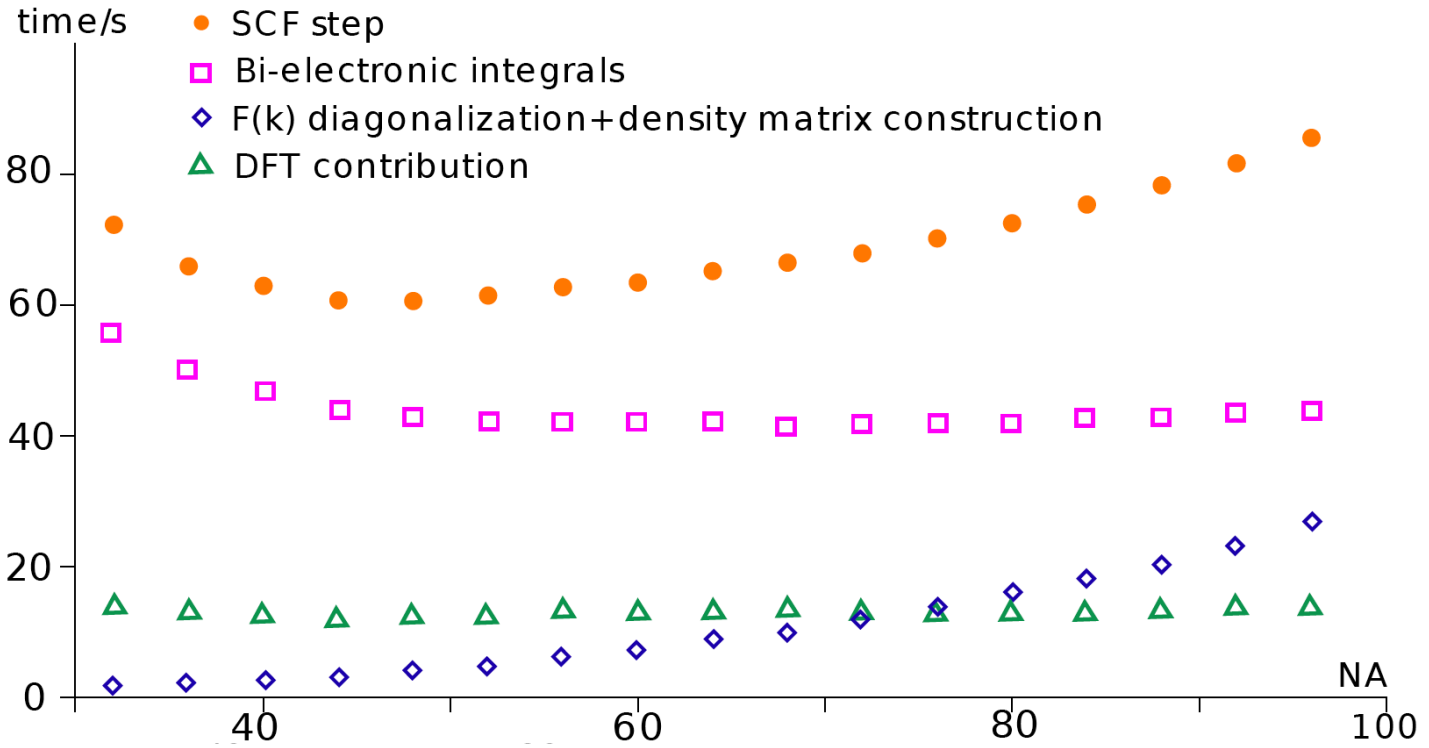

SCF cost increases (slowly) for three reasons:
1- Diagonalization scales linearly with N_S.
2- AO→Bloch→SACO and back transformations to AO basis for building the density matrix scale close to N(AOs)*N(AOs).
3-Overhead for symmetry analysis increases with N_S

* Noël, D'Arco, Demichelis, Zicovich-Wilson, Dovesi; J. Comput. Chem., 2010, 31, 855-862

Nanotubes

Time Scaling

- NANORE (SWCNTRE): build a (n_1,n_2) nanotube from the structure of another one

"old" nanotube unrolled and re-rolled according to a new ***R*** vector, with minor modifications to the structure.

***EXAMPLE*: geometry optimisation of imogolite**

$Al_2(OH)_3SiO_3OH$, tubular hydrated aluminosilicate

(thick slabs, large systems, tube and slab geometries very different)

starting structure for the optimisation
(the optimised slab or a previously optimised tube)

	ATOMS	Beginning	Number of SCF+gradient	ΔE	δE
(8,0)	224	(9,0)	22	-47.8	-8.0
(9,0)	252	(10,0)	20	-52.1	-4.2
(10,0)	280	slab	**46**	-52.6	-236.6
(11,0)	308	(10,0)	19	-51.8	-2.4
(12,0)	336	(11,0)	16	-50.8	-1.5

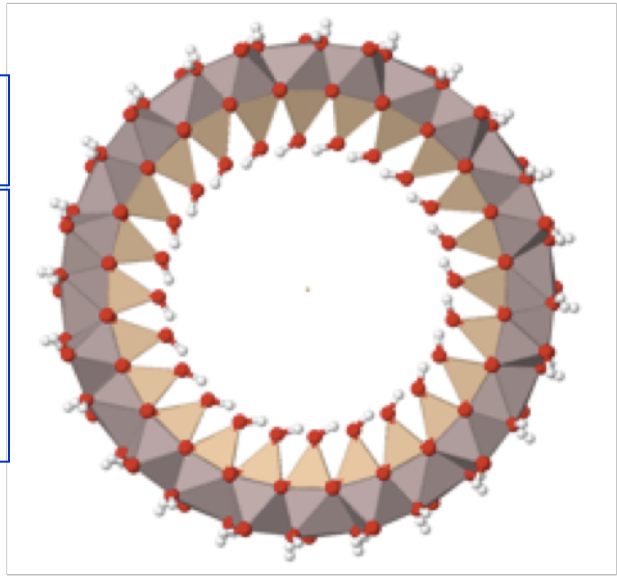

ΔE: Energy difference with respect to slab, kJ/mol per fu

δE: Energy relaxation after rigid unrolling and re-rolling , kJ/mol per fu

* Demichelis, Noël, D'Arco, Maschio, Orlando, Dovesi; submitted for publication

Nanotubes

Inorganic Nanotubes: the Case of Chrysotile

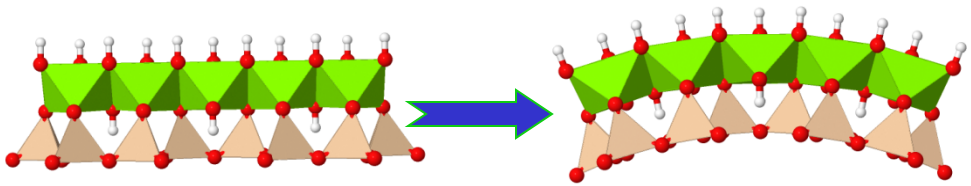

FIRST AB INITIO SIMULATION OF SINGLE LAYER CHRYSOTILE (smallest fibre in the nature ~1000 atoms in the unit cell)

"White" asbestos: wrapping of lizardite - phyllosilicate, $Mg_3Si_2O_5(OH)_4$

-brucite-type octahedral sheet (MgO_6 octahedra sharing edges)
-tetrahedral sheet (vertices-sharing SiO_4 tetrahedra forming hexagonal motif)

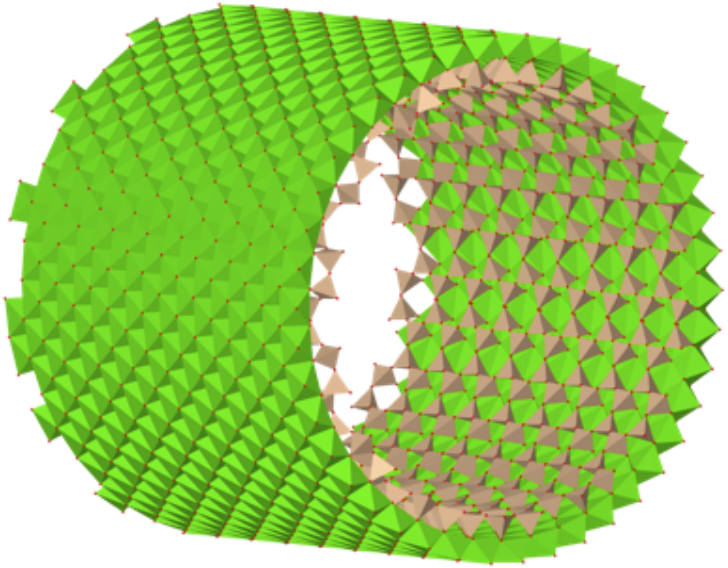

Brucite-like slab : lattice parameter 5.43 Å
$SiO_3(OH)_2$ slab : lattice parameter 5.32 Å
Lizardite slab : lattice parameter 5.37 Å

The **misfit** might be one of the main responsible for chrysotile **curling**. Octahedral external wall is allowed to expand and tetrahedral wall to contract.

* D'Arco, Noël, Demichelis, Dovesi; J. Chem. Phys., 2009, 131, 204701

FULLERENES

Input again: general!!

```
SLAB
77
2.4612
1
6  -0.33333333333 0.33333333333 0.
FULLE
2 2
IH
ICOSA
...
```

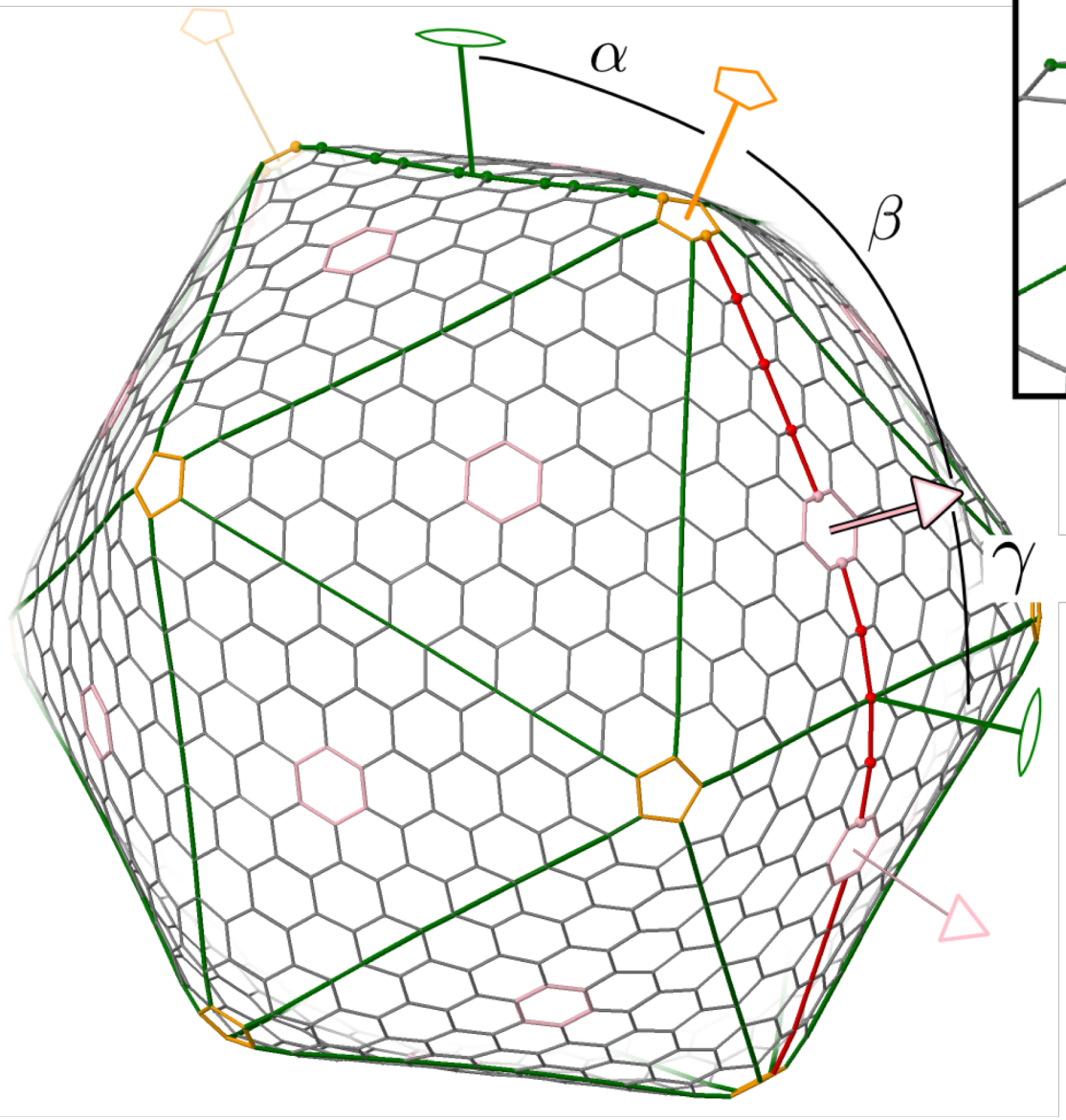

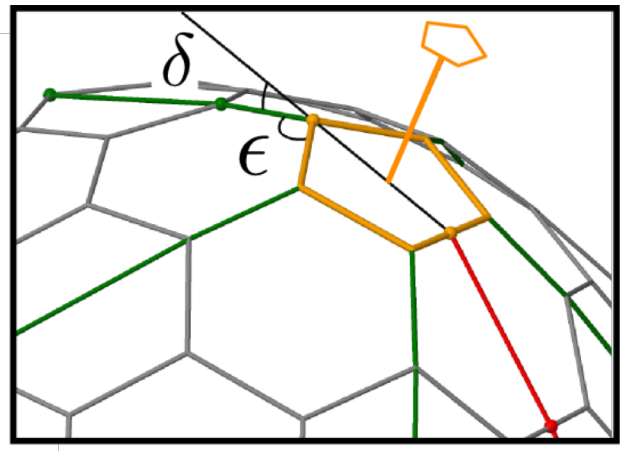

Some (in pink) hexagons (or pentagons in orange) cannot change their orientation; it is fixed by symmetry

C1500
fullerene

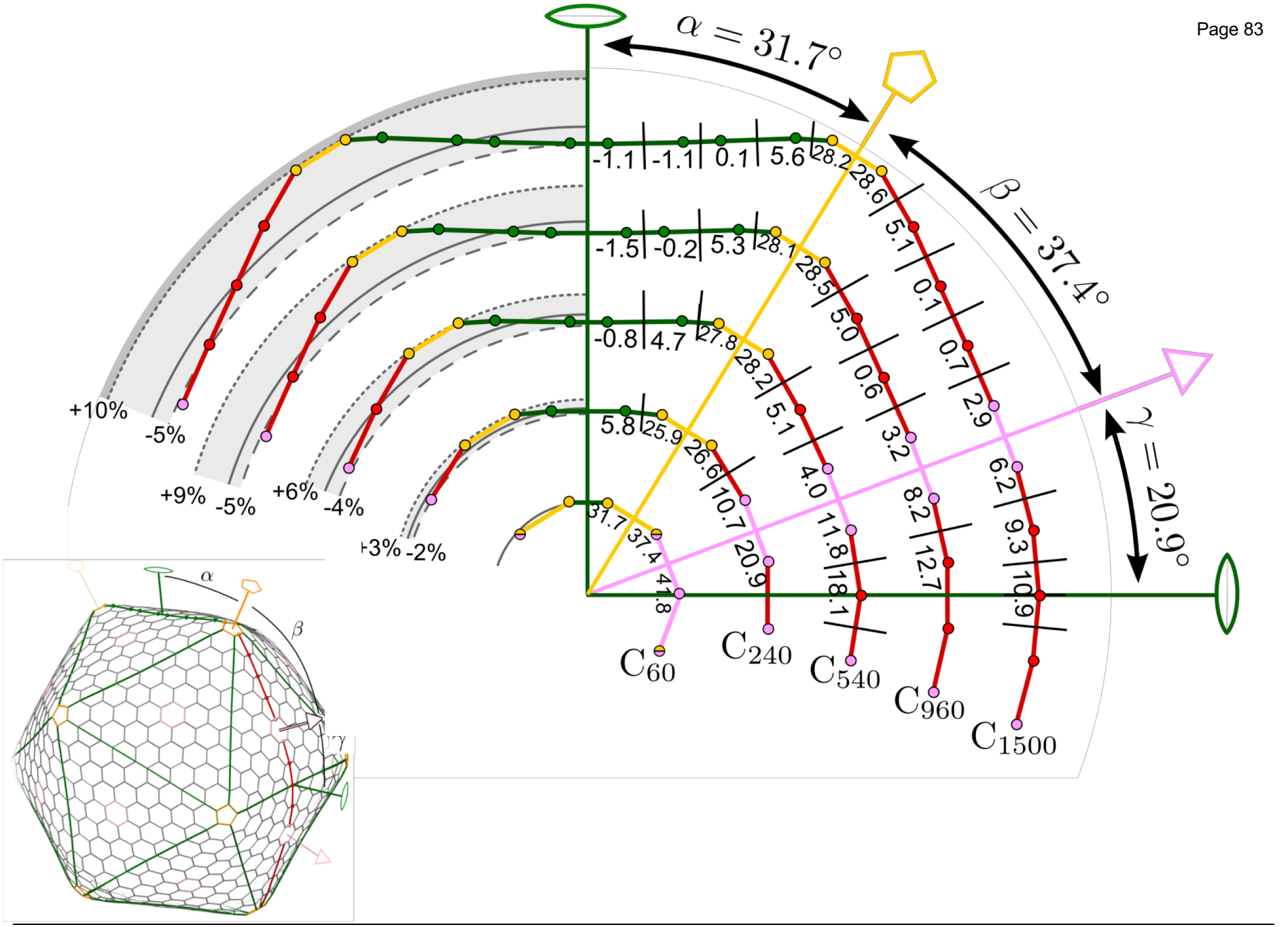
$\alpha = 31.7°$
$\beta = 37.4°$
$\gamma = 20.9°$
+10%
-5%
+9%
-5%
+6%
-4%
+3%
-2%
-1.1 -1.1 0.1 5.6 28.2
-1.5 -0.2 5.3 28.1
-0.8 4.7 27.8
5.8 25.9
37.7
28.6 5.1 0.1 0.7 2.9
28.5 5.0 0.6 3.2
28.2 5.1 4.0 11.8 18.1
26.6 10.7 20.9
37.4 41.8
6.2 9.3 10.9
8.2 12.7
C_{60}
C_{240}
C_{540}
C_{960}
C_{1500}
α
β
γ

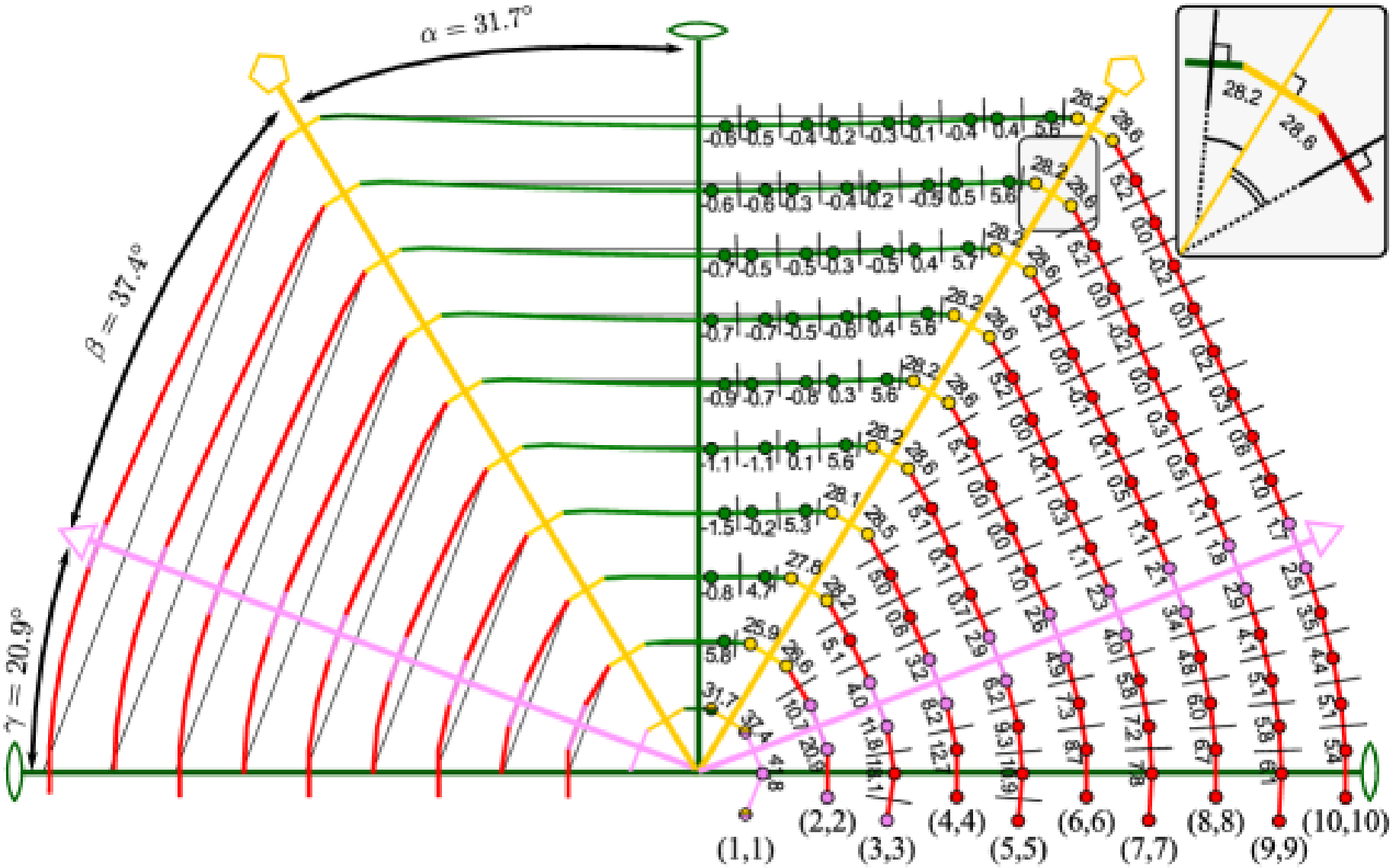
$\alpha = 31.7°$
$\beta = 37.4°$
$\gamma = 20.9°$
(1,1)
(2,2)
(3,3)
(4,4)
(5,5)
(6,6)
(7,7)
(8,8)
(9,9)
(10,10)

Comparison of optimized structures

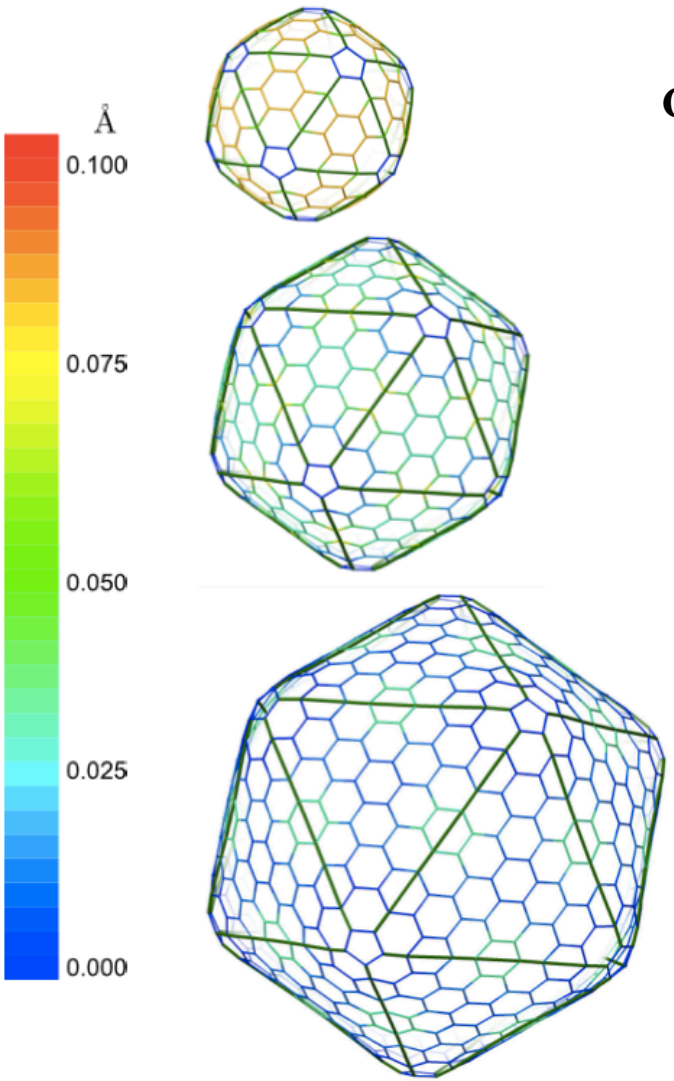

C240

C540

Each fullerene is compared to the C1500. The center of pentagons have been taken as reference.

C960

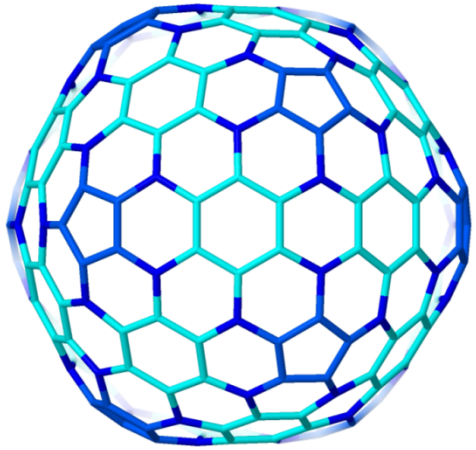

(2,2)

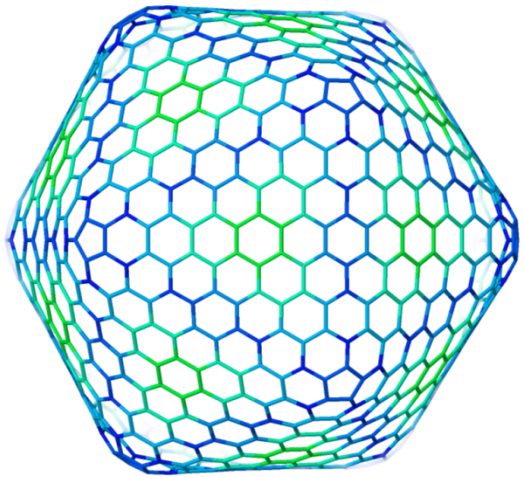

(4,4)

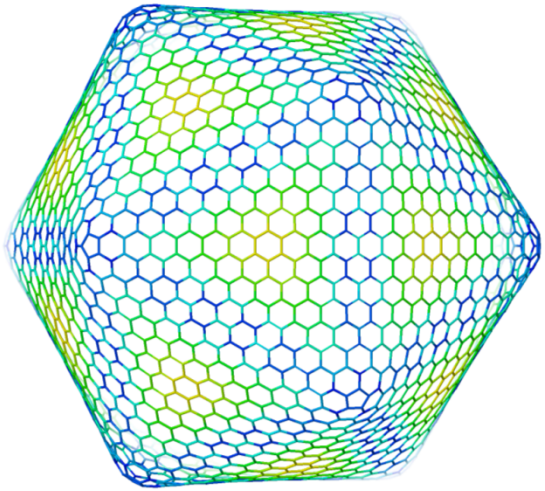

(7,7)

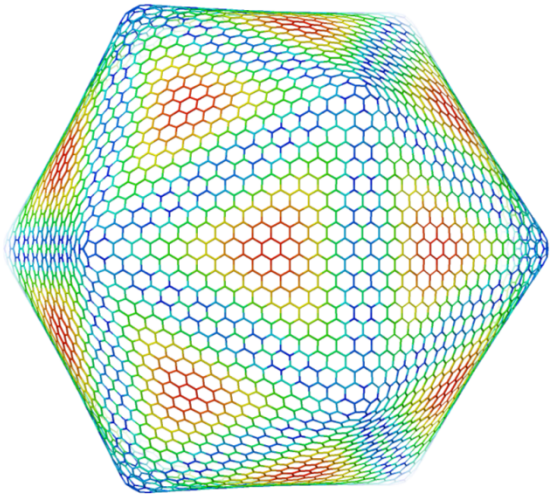

(10,10)

FULLERENES: size of the matrices

(n,n)	n_{at}	N_{at}	N_{AO}	S_{FIRR}	S_{FRED}	R_1	R_2	R_4
(1,1)	1	60	840	1759	169'980	97	401	22
(2,2)	3	240	3360	6707	716'130	107	1683	23
(3,3)	6	540	7560	14570	1'609'020	110	3923	23
(4,4)	10	960	13440	25377	2'847'690	112	7118	23
(6,6)	21	2160	30240	55661	6'362'370	114	16429	24
(8,8)	36	3840	53760	97559	11’260’170	115	29625	24
(10,10)	55	6000	84000	151071	17’541’090	116	46707	24

n_{at} = number of irreducible atoms, N_{at} = number of atoms,

N_{AO} = number of AO

S_{FIR} (S_{FRED}) = size of the irreducible (reducible) **compact** Fock matrix.

R_1, R_2 and R_4 = S_{FRED}/S_{FIRR} , N_{AO}^2/S_{FIRR} and N_{AO}/MAX_{IR}.

N_{op} = 120

N_{IR} = 10

	t	(1,1)	(4,4)	(6,6)	(8,8)*	(10,10)*
A.	*init*	26.36	64.92	184.54	418.64	825.41
"	*over*	81.40	8.11	22.36	56.73	135.85
B.	*pole*	326.15	6.64	14.76	26.51	40.77
"	*biel*	8.34	154.46	578.06	1141.61	1885.74
"	*mono*	0.02	4.45	21.98	68.70	166.01
C.	*fock*	0.16	7.71	18.91	36.27	56.31
D.	*diag*	0.1	2.51	26.20	183.42	729.50
E.	*dens*	1.23	93.02	233.02	441.63	740.14
F.	*dft*	5.50	55.16	126.18	437.99	702.36
	TOT_{cyc}	15.67	323.97	1019.14	2336.16	4320.87
	TOT_{SCF}	1265.23	6552.43	20589.74	47198.57	87378.66
	grad	83.99	1253.55	3191.33	10088.28	16170.70

Time (in seconds): ONE CORE

construction of symmetry group and transformation matrices (*init*), construction of the overlap matrix (over), calculation of multipole (*pole*), bi- (*biel*) and mono- (*mono*) electronic integrals, transformation of f into F (*fock*), Fock matrix diagonalization (*diag*), construction and back transformation of the density matrix (dens), calculation of the electron density over the DFT grid (*dft*), a single SCF cycle (TOT_{cyc}, from B. to F.), the entire SCF procedure (TOT_{SCF} , 20 SCF cycles considered), calculation of the gradient for geometry optimization (*grad*). Calculations from (7,7) on (marked with an asterisk) were performed using the "low memory" option.